Scholars' Mine

Masters Theses   Student Theses and Dissertations

Spring 2018

Cellular hitchhiking via injectable microparticles

Daniel Smith

Follow this and additional works at: https://scholarsmine.mst.edu/masters_theses

Part of the Chemical Engineering Commons

Department:

Recommended Citation

CELLULAR HITCHHIKING VIA INJECTABLE MICROPARTICLES

by

DANIEL SMITH

A THESIS

Presented to the Faculty of the Graduate School of the

MISSOURI UNIVERSITY OF SCIENCE AND TECHNOLOGY

In Partial Fulfillment of the Requirements for the Degree

MASTER OF SCIENCE IN CHEMICAL ENGINEERING

2018

Approved by

Dr. Sutapa Barua, Adviser

Dr. Dipak Barua

Dr. Jee-Ching Wang

PUBLICATION THESIS OPTION

This thesis consists of the following two articles, formatted in the style used by the Missouri University of Science and Technology:

Paper I: Pages 9-39 are intended for submission to Acta Biomaterialia Journal

Paper II: Pages 40-62 have been submitted to NanoLIFE Journal

ABSTRACT

Tissue engineering is a process of developing new tissues in a host. Tissue engineering draws upon revitalizing damaged tissues that otherwise would not heal completely from the body's natural response. To augment the body's natural response to impairment, cells can be transplanted to the afflicted area to boost the healing response. Implementing these cells onto scaffolds and transplanting them into the body improves the healing response dramatically. Tissue regeneration improves when a biodegradable scaffold is used in conjunction with cells to augment the body's healing response. Microparticles provide a surface that can mimic the environment cells perceive *in vivo*, allowing cells to proliferate and grow on the microparticle surface optimally. When these microparticles are transplanted into the body, the accompanying cells transition into the host tissue as the microparticles degrade. Proteins comprising the extracellular matrix (ECM), like collagen, fibronectin, and laminin, are used to facilitate cell binding to substrates, whether a biomaterial material *ex vivo* or an enzyme *in vivo*. Functionalizing the surface of microparticles with ECM proteins improves the adherence of cells which increases the area of tissue regenerated. When cells bind to ECM proteins on a biomaterial, a cascade of signals is initiated which communicates to the cell to spread on the surface of the biomaterial and begin the process of mitosis, leading to proliferation. Cationic polymers have also been shown to improve cell-surface interactions. Functionalizing particles with cationic polymers and extracellular matrix proteins provides a surface optimized for cell attachment and spreading.

ACKNOWLEDGMENTS

Firstly, I'd like to thank my adviser, Dr. Sutapa Barua, for being the motivating and driving force behind my course of study. Dr. Sutapa has always believed in my abilities and has been willing to walk an extra mile to help me succeed. Without her patience, resolve, and faith, I could not have completed this thesis. For that I am eternally grateful to have her as my adviser, her guidance and foresight have taught me many lessons on not only how to be a successful researcher, but also leading a fruitful and promising life.

Secondly, I'd like to thank my advising committee: Dr. Jee-Ching Wang and Dr. Dipak Barua, for providing support whenever asked and taking precious time out of their schedules to assist me in this endeavor.

I'd also like to thank my father and mother, Michael and Kay Smith, as well as my brother, Matt, and my sister, Angie, for their continued support and love throughout all my efforts and passions in life, no matter how extreme or difficult. For always lending an ear when needed and providing a hand to help when asked; I will always be grateful for the love of my family.

Lastly, I'd like to thank my friends I've made at Missouri S&T. They have been a family to me and made Rolla feel like home.

TABLE OF CONTENTS

SECTION

LIST OF ILLUSTRATIONS

LIST OF TABLES

NOMENCLATURE

Symbol	Description
BCA	Bicinchoninic Acid
BSA	Bovine Serum Albumin
CAM	Calcein acetoxymethyl (AM)
DAPI	4',6-diamidino-2-phenylindole
EDC	1-Ethyl-3-(3-dimethylaminopropyl)carbodiimide
HUVEC	Human Umbilical Vein Endothelial Cells
MES	2-(morpholino)ethanesulfonic acid
NHS	N-hydroxysuccinimide
PCL	Polycaprolactone
PEG	Polyethylene Glycol
PLGA	Poly(lactide-co-glycolide) acid
PLL	Poly-l-lysine
PG	PLGA-Gelatin
P2	PLGA-PLL
P2G	PLGA-PLL/Gelatin
SN	Supernatant

SECTION

1. INTRODUCTION

Tissue engineering is a quickly developing field that has the potential to change the face of medicine. Engineering tissues requires the use of both cells and non-cytotoxic materials. These materials can be either synthetic, natural, ceramic, or metallic. Metallic and ceramic materials are best used in joint replacement procedures, such as hip or knee replacement, because these joints should last for at least 10 years or more. Additionally, metallic and ceramic materials have larger Young's moduli and thus are more resistant to stress and strain, which is required in large joints. However, metallic and ceramic materials are still prone to inflammation and immune response leading to implant degradation over time. Since new tissue is not formed in these implants the body will eventually reject the implant requiring the implant to be removed and replaced. While metallic and ceramic biomaterials are stronger and more resilient, natural or synthetic scaffolds show promise in permanent remedies for biological damage.

1.1 SYNTHETIC BIOMATERIALS

Synthetic biomaterials are composed of polymers with a range of properties. Synthetic scaffolds are robust and versatile and can be used in a variety of tissue regeneration processes. Most synthetic scaffolds are polymeric, with polyesters being common, and can be fashioned into constructs similar to natural scaffolds, however, synthetic materials can range from weak to strong mechanical properties, long to short degradation times, and bioinert to biodegradable, while maintaining low to zero cytotoxicity [1]. Synthetic scaffolds benefit from stronger mechanical properties, resistance to dangerous biological environments, control over degradation rate, and are

easily modifiable and tunable compared to natural biomaterials [2]. When considering tissue regeneration, the strength of the biomaterial is of pivotal importance to support the tissue they encompass in order to prevent plastic degradation, or irreversible degradation, or breakage. Depending on which tissue is being regenerated will influence what material is chosen as a scaffold. For example, the Young's modulus of bone is 338.3 MPa [3] whereas cartilage tissue has a Young's modulus of 0.45 to 0.8 MPa [4]. To regenerate either of these two tissues, the biomaterial chosen should have a Young's modulus close to that of the tissue. In addition, the degradation rate of the biomaterial must be chosen such that the material degrades at a similar rate that tissue regenerates. Tissues in the body rejuvenate at different rates and this requires that a biomimetic scaffold degrade at a rate that matches rejuvenation of the damaged tissue. The degradation rate should match the proliferation rate of the cells composing the damaged tissue such that a seamless incorporation of implanted cells occurs. However, most synthetic scaffolds do not readily associate with cells like their natural counterparts, which is a critical aspect of tissue engineering. Synthetic scaffolds are typically hydrophobic, carrying a net negative charge which is known to repel cells due to their net negative charge around the plasma membrane [5]. To effectively achieve cellular attachment to synthetic scaffolds, surface functionalization is typically required. Scaffolds are functionalized through physical adsorption [6], bioconjugation [7], or plasma polymerization [8] with extracellular matrix proteins [8-10] or cationic polymers [11-14]. Extracellular matrix proteins contain specific amino acid sequences that anchorto receptor proteins on the cell membrane [15], whereas cationic polymers utilize electrostatic interactions to associate with cellular membranes [16]. The biomaterial most advantageous for which tissue is engineered

depends on the recovery rate of the tissue. Bone, cartilage, skin, muscle, and heart tissue each have unique regeneration responses. Each of these tissues use specific signal cascades to deliver different types of cells and growth factors at certain times in their regeneration process. Due to the varied wound response of each tissue, a biomaterial to regenerate these tissues must be carefully chosen. A variety of materials are available for tissue engineering such as polycaprolactone (PCL), poly(glycolic acid) (PGA), poly(lactic acid) (PLA), poly(methyl methacrylate) (PMMA), polystyrene, and Poly(lactic-co-glycolic) acid (PLGA). PCL has a long degradation time and is useful for applications where slow, continual repair or drug delivery is required. PGA is a hydrophilic polymer that has been used for synthetic, biodegradable sutures due to its quick degradation time. PLA is a hydrophobic polymer, owing to the methyl pendant group off its main chain, and has been used for stents for blood vessel stenosis [17]. PMMA is a bioinert material with powerful mechanical strength and has been used as bone cement. Polystyrene particles have been used to study the effect of different shapes of micro and nanoparticles in relation to their uptake in cancer cells [18]. PLGA is a versatile biomaterial which is FDA approved and has been used in drug delivery, and tissue regeneration [12, 19]. PLGA degrades through hydrolysis into lactic and glycolic acid. Lactic acid is naturally produced during anaerobic cellular respiration and is excreted as waste. Glycolic acid is an extremely water-soluble molecule; thus, it is easily removed from the body as waste in urine [20]. PLGA is versatile in that it can be fabricated into fibers [21], constructs of varying dimensions by sintering [22], disk [18], rods [23], or particles [24]. PLGA is a prime contender for tissue engineering applications because of its degradation rate, mechanical strength, and ease of

functionalization. PLGA degradation rate can be controlled by varying the ratio of glycolic acid to lactic acid in the copolymer. When composed of a 50/50 mix of the two comprising polymers, PLGA experiences its quickest degradation rate; undergoing complete degradation within 4 weeks *in vivo*. By increasing the molar ratio of lactic acid in PLGA, the degradation rate can increase to 7 months, whereas increasing the glycolic acid ratio increases degradation rate to at most 5 months. Therefore, PLGA can be used in a wide variety of tissue regeneration applications. Additionally, PLGA naturally consists of carboxyl groups due to the presence of glycolic acid. These carboxyl groups allow PLGA to be modified with proteins through amine coupling in bioconjugation processes. Modifying the surface of PLGA with proteins increases the ability for cells to associate with the biomaterial enabling augmented tissue regeneration. Using biomaterials for tissue regeneration is important because severely damaged tissues will not undergo complete repair like broken bones in elderly patients, or severe burns. However, the infusion of transportable microparticle devices for cell delivery into damaged tissues offers a new paradigm for tissue regeneration.

1.2 NATURAL BIOMATERIALS

Natural scaffolds are comprised of materials naturally found in the body. These materials typically comprise the extracellular matrix network, which anchors cells together as tissues, as well as structural and sensing components of the plasma membrane on cells. Proteins are a typical natural biomaterial used in tissue regeneration. Proteins are interesting molecules because they are synthesized in a cell, from translated messenger ribonucleic acid (mRNA), and are built in a structural hierarchy. The mRNA is translated

by ribosomes into amino acids, which are the building blocks of protein. There are 20 common amino acids which form all proteins found in the body. These amino acids are linked together in a chain by peptide bonds, which forms the first-degree structure of proteins. Depending on the amino acid profile of the peptide chain, the peptide conforms into one of two secondary structures: an alpha helix or beta sheet. The alpha helix and beta sheet are stabilized through hydrogen bonds between successive amino acids. These secondary structures associate with each other through hydrogen bonding as well as disulfide bonds between cysteine residues to form a tertiary structure, which is the three-dimensional representation of a protein. This tertiary structure undergoes folding and modification to form a functional protein. Furthermore, these tertiary structures will associate to form a quaternary structure, which is at least two tertiary proteins binding together through disulfide bonds and hydrogen bonding.

Natural scaffolds are derived from materials occurring naturally *in vivo* such as, hyaluronan [10], chitosan [25], chondroitin-6-sulfate [26], collagen [27], and many others [28] and have been prepared as films [29], hydrogels [30], fibers [31], and particles [32]. Chitosan is an interesting biomaterial considering it is an amino polysaccharide consisting of N-acetyl-D-Glucosamine. Chitosan is formed from the deacetylation of chitin, a hard material used by shrimp, crabs, and other shellfish for their shells. The deacetylation step allows for chitin to polymerize with D-glucosamine *via* glycosidic bonds, forming the cationic polymer chitosan. Due to the large number of amino groups littered on the backbone of chitosan, it has large potential as a tissue engineering material. The amino groups will carry a positive charge at physiologic pH (7.4) which will help associate with the negatively charged plasma membrane of cells. In addition, chitosan is

mucoadhesive and thus can bind to mucus membranes [33]. Chitosan is especially useful as a hydrogel [34] since it can incorporate numerous bioactive compounds through electrostatic interactions and amide bonds. Nucleic acids, like DNA, are a promising natural material for regenerative medicine. DNA has been formed into many shapes and structures and is a potential nanomaterial for drug delivery, biomarkers, and shape controlling of hydrogels [27]. However, DNA is limited in tissue engineering as it is difficult to fabricate into large structures. Additionally, the net negative charge of DNA is a natural repellent of the plasma membrane, limiting its ability to associate with cells. These biomaterials show virtually no cytotoxicity and many compose the extracellular matrix or are involved in cell anchoring, spreading, and communication [14, 35]. In this manner, natural materials are advantageous for tissue engineering because they naturally associate with cells and stimulate cellular proliferation. However, natural biomaterials, especially proteins, are subject to hydrolysis and enzymatic degradation *in vivo*. Additionally, natural materials suffer from limitations in synthesis. Many natural materials must be maintained in solutions that are at or near physiologic pH, otherwise they will degrade. Proteins are dependent on temperature to maintain proper structure, otherwise known as their native conformation. Above 37°C proteins degrade into their amino acid constituents and lose their function, likewise, materials made solely out of proteins can not withstand temperature fluctuations. Natural scaffolds also suffer from weaker mechanical properties and quicker degradation in atypical somatic environments, such as the acidic pH environment at wound sites, relative to synthetic biomaterials. Thus, natural scaffolds are a useful tool for tissue regeneration, however, their capacity is limited when used on their own.

1.3 TISSUE ENGINEERING

In the presented study, synthetic biomaterials were coupled with materials derived from naturally occurring proteins in the body for the attachment of endothelial cells. Endothelial cells line the lumen of blood vessels and are defined as either vascular or lymphatic depending on whether they are in contact with the blood or lymph, respectively. These cells diffuse nutrients and oxygen from the blood to tissues throughout the entire body as endothelial cells line the entire vasculature. Additionally, they act as a mediator for immune cells to traverse the body and infiltrate wounded and diseased tissues. Blood vessels are responsible for many functions like fluid filtration in the kidneys, maintaining homeostasis, and delivering hormones. When a tissue, such as skin, incurs damage, blood vessels are typically damaged as well, which is apparent when someone bleeds. By using biomaterials to deliver endothelial cells to damaged tissues, an increased response to wound repair is expected. These cells participate in angiogenesis, which is the formation of new blood vessels. Considering that blood vessels are responsible for delivering oxygen and removing wastes from tissues, delivering these cells using biomaterials is important in regenerating tissue. For example, when someone suffers from a heart attack there is a chance that acute myocardial infarction can develop. When a patient suffers from acute myocardial infarction part of the tissue in the heart dies and is repaired by fibrosis. Fibrosis occurs when scar tissue forms to repair a wound site. It is possible that stimulating tissue which has suffered myocardial infarction with endothelial cells will improve wound repair and prevent scar tissue formation and fibrosis.

Li et. al. used trophoblast and mesenchymal stem cells to augment repair of myocardial infarction in a mice model [36]. The group instigated myocardial infarction, colloquially known as a heart attack, in a mouse, then applied stem cells derived from embryonic blastocysts. Trophoblast and mesenchymal stem cells were successfully delivered to the heart and did reduce the area of infarction, however, only 8% of the stem cells successfully engrafted into the tissue and proliferated. A majority of the cells did not transplant to the target location and were flushed away by the mouse's excretory system. Low engraftment rates are a pivotal issue in cell-based therapies. Many regenerative therapies suffer because cells do not efficiently adhere to the wounded tissue. These cells have difficultly incorporating into tissues of interest because the body's blood vessels are constantly pushing fluids through every system in the body. Cells get flushed away during this cycle. To alleviate excretion of cells biomaterials are being developed which can target wounded tissues and bind cells. Using biomaterials as a mediator for tissue regeneration improves cell engraftment in damaged tissues. Additionally, these biomaterials can be functionalized to bind specific types of cells as well as target specific tissues, rather than the "shotgun" approach of administering cells in a wholesale fashion. Furthermore, the advent of microparticles facilitates ease of administration through minimally invasive surgical procedures. Also, microparticles are versatile and can be applied to virtually all tissues and are modular in that they can be functionalized to enable attachment of any cell type. The present investigation elicits the potential of these microparticles such that their surface can be functionalized through bioconjugation or physical adsorption using either extracellular matrix derived proteins, like gelatin, or polycationic polymers like poly-l-lysine (PLL).

PAPER

I.   **PLGA MICROPARTICLES AS VEHICLES FOR CELL TRANSPORT**

ABSTRACT

Tissue engineering offers promising solutions for the future of regenerative medicine. Current technology focuses on metallic or ceramic implants for replacement therapy, direct application of cells to damaged tissues, or large constructs or hydrogels. Particles offer a promising approach to tissue regeneration, however, many studies have been limited to small particles sizes (<50 µm) which limits the extent to which cells can attach and be modelled as a biomimetic device. Here, the efficacy of a simple flow-focusing device coupled with the single emulsion solvent diffusion technique to fabricate poly(lactic-co-glycolic) microparticles for attachment of human umbilical vein endothelial cells (HUVECs) is demonstrated. PLGA microparticles measured at 122 ± 40.4 µm in diameter and reached up to 156 ± 39.9 µm in coated formulations. Zeta potential ranged from -16.7 to -35.1 mV. Coating efficiency ranged from $30.6 \pm 1.51\%$ to $76.8 \pm 4.94\%$. Particles were assessed for cell binding potential using confocal and light microscopy as well as flow cytometry. A mixture of cationic polymer and extracellular matrix adsorbed on the surface of the microparticles resulted in the most cells attaching to the surface.

1. INTRODUCTION

Biodegradable and biocompatible materials offer an effective channel for advancing regenerative medicine and tissue engineering. Common polymers in use are poly(lactic-co-glycolic acd) (PLGA) [1-3], poly(lactic acid) (PLA) [4, 5], polycaprolactone (PCL), and polyethylene glycol (PEG) [6] and are FDA approved for use *in vivo* [7]. One of the barriers for biomaterials to overcome is cell attachment and delivery. Tissue engineering requires delivery of cells to a target site to induce healthy regeneration and prevent hazardous scar tissue formation. Tissues with large scar areas are prone to malfunction and increased risk of further injury. In fact, a wound area which encompasses a large fraction of tissue surface area can not fully repair by natural mechanisms [8], total repair requires the use of a biomaterial to augment the regeneration response. Biodegradable materials are chosen for their degradation rate, mechanical properties, and surface characteristics. Their unique ability to interact with the human body without producing a cytotoxic or immune response facilitates their use as a scaffold for culturing cells. PLGA is a versatile biomaterial which degrades due to hydrolysis in as little as two weeks [9]. Current studies demonstrate the efficacy of PLGA as an instrument for regenerating cardiac [10], nervous [11, 12], hepatic [13], cartilage [14], and skin tissue [15]. However, current studies have not thoroughly investigated the capability for microparticles to induce tissue regeneration, especially in skin tissue reconstruction. Particles are easily distributed *in* vivo by minimally invasive surgical techniques, rather than open surgery for implants and large constructs. This reduces the inherent risk to patients and provides a safe solution to tissue repair. Certain formulations of PLGA degrade within 2-4 weeks once implanted *in vivo* [16] which is ideal in the regeneration of severe wounds. The

initial wound response *in vivo* where the majority of cellular repair including vascularization and mending of the wound gap takes place within a month of the initial wound incursion [17].

A major limitation in improving tissue regeneration and repair in the body is cellular attachment to biomaterials. Extracellular matrix is a critical component for cell survival, proliferation, and attachment. The extracellular matrix not only functions as an anchor for cells to adhere to and spread on, but also acts as an information boulevard for cells to communicate with each other through signaling molecules. Synthetic biomaterials lack these extracellular domains that cells recognize and thus require modification for healthy cell attachment. When an extracellular matrix is lacking in a cell's environment, programmed cell death, like anoikis or apoptosis, can occur. Thus, biomaterials are functionalized with extracellular matrix proteins, such as fibronectin [18], collagen [5], or laminin [19], or cationic polymers like chitosan [20, 21] or poly-l-lysine (PLL) [22].

Endothelial cells line blood vessel walls and provide an intricate super highway for nutrient and gas delivery throughout the body. Thus, endothelial cells are found in most tissues of the body including organs, muscles, and bones. Curiously, in skin only the dermis is vascularized, whereas the epidermis receives nutrients through diffusion from the dermis and from the environment. Endothelial cells are crucial for maintaining this homeostasis as skin relies on dense vascular networks to deliver excesses of nutrients such that the epidermis is properly maintained. However, in severe burns, abrasions, or ulcers, the skin loses its ability to completely regenerate leaving the formation of a scar. The scar tissue formed consists of extracellular matrix proteins aggregated to seal the wound site. However, the use of biomaterials as vehicles for cellular delivery to augment

tissue repair response has the potential to prevent malignant bodily responses. Delivery of endothelial cells to the wound site would increase vascularization marking an improvement in vital nutrient delivery. Transporting cells effectively has proved challenging since biomimetic scaffolds typically require extensive surface modification in the form of plasma polymerization [5, 23, 24] conjugation chemistry [2,14], or physical adsorption [11], while the literature seldom mentions endothelial cell attachment to microparticles.

Herein is described a simple but effective method for endothelial cell attachment. PLGA microparticles were fabricated using a modified version of the single emulsion solvent-evaporation method utilizing a proprietary flow-focusing device. Additionally, particles were surface functionalized for cellular attachment by physical adsorption of PLL, gelatin, or a combination of both. Finally, particles were assessed for cell attachment and potential.

2. MATERIALS & METHODS

2.1 MICROPARTICLE SYNTHESIS

The solvent diffusion method was used with a simple flow-focusing apparatus to synthesize polymer microparticles. Firstly, an organic solution was formulated by dissolving 300 mg of Poly(D,L-lactide-co-glycolide) (PLGA; Acros Organics, ~19 kDa) in 4.5 ml of ethyl acetate (Fisher Scientific). An aqueous solution of 1 % (w/v) polyvinyl alcohol (PVA; Sigma-Aldrich, 30-70 kDa) was formed by dissolving PVA in reverse osmosis (RO) water. A flow-focusing apparatus was assembled with 5 and 10 ml syringes, a two-syringe pump (kdScientific, KDS-200), plastic tubing, a Pasteur pipette, and a stir plate. The 5 and 10 ml syringes were completely filled with the PLGA and 1% PVA solutions, respectively; these represent the organic and the aqueous carrier streams of the flow-focusing apparatus.

By using an equal drive block velocity on both syringes, the two streams were injected into the Pasteur pipette at a 7:10 flow rate differential. With careful adjustments, gently forcing the organic stream tubing into the pipette neck produced regularly-sized organic droplets surrounded by the aqueous carrier stream in the pipette capillary. The Pasteur pipette was positioned vertically above 100 ml of the 1 % PVA solution (stirring at approximately 250 rpm) such that the pipette tip was just submerged near the center of the solution's vortex whorl. For 10 minutes of injection, the organic droplets were dispersed into the continuous aqueous phase. The Pasteur pipette was then removed, and the emulsion was stirred for an additional 15 minutes. The mixture was left undisturbed overnight (> 18 hours) to allow for evaporation of residual ethyl acetate at room

temperature. PVA was removed by centrifugation at 7,000 rcf, followed by five washes with RO water. Microparticles were then lyophilized, weighed, and stored at 4°C.

2.2 MICROPARTICLE CHARACTERIZATION

The size and surface topography of PLGA microparticles were analyzed with SEM at 1-10 kV (Hitachi S-4700) and stereo microscopy (Hirox KH-8700). Particle size and shape were also visualized with bright field microscopy (Nikon Eclipse E400). The microparticle surface charge was measured in water and phosphate buffer saline (PBS; Fisher Scientific) with dynamic light scattering (DLS; Malvern NanoSeries Zetasizer ZS90). DLS measurements were performed at 25°C in disposable capillary cells (Malvern) using the backscattering detection at 90°. The zeta potential was measured for 20 successive runs. Data was analyzed using means and standard deviations of three measurements.

2.3 SURFACE COATING OF MICROPARTICLES

Poly-l-lysine (Sigma, PLL, MW ~150,000-300,000 Da) and gelatin from bovine (Sigma, bloom ~ 225-300) were physically adsorbed onto the surface of PLGA microparticles to increase cell-particle interactions. Briefly, 35 mg of microparticles was weighed and added to three centrifuge tubes for PLGA-Gel (PG), PLGA-PLL (P2), and PLGA-PLL/Gel (P2G) particles. All tubes were coated in Sigmacote® (Sigma) to minimize product loss. For PG particle formulations, 75 µl of a 0.32% w/v solution of gelatin in RO H_2O was added, for a total of 240 µg of gelatin. P2 formulations received 240 µl of a 0.1% w/v PLL solution, P2G particles 45 and 96 µl of gelatin and PLL stock,

respectively, for a total of 240 μg of protein at a ratio of 40/60 PLL/Gel. Samples were

incubated at 37°C and rotated at 20 rpm for 4 hours. Particles were then centrifuged at

4,696g for 20 minutes and washed 3 times with RO H$_2$O. Microparticles were then

lyophilized, weighed, and stored at 4°C.

2.4 SURFACE COATING QUANTIFICATION

To effectively determine the amount of PLL and gelatin adsorbed on the surface of

PLGA microparticles, nuclear magnetic resonance (NMR) analysis was employed.

During the washing of coated particles, the supernatant was collected for NMR analysis.

The supernatant was frozen and lyophilized until constant weight was achieved. This

product was then diluted in 700 μl of deuterium oxide (D$_2$O) and analyzed using 1H

NMR (INOVA 400 MHz FT/NMR, Varian, Inc.). Spectral data was collected and

analyzed for the integral area under characteristic peaks for PLL and gelatin. The area

under the characteristic peaks was used to calculate total protein content in the

supernatant samples using a standard curve. Percent adsorption efficiency was then

determined using the following equation:

$$\%AE = \frac{Initial\ protein - Sample\ protein}{Initial\ Protein} * 100\% \qquad (1)$$

2.5 CELL ATTACHMENT, PROLIFERATION, & QUANTIFICATION

Human Umbilical Vein Endothelial Cells (HUVEC, Lonza) were maintained in

Endothelial Growth Medium (PromoCell), supplemented with 2% v/v fetal calf serum

(FCS), 1 μg/ml hydrocortisone, 0.1 ng/ml human epidermal growth factor, 1 ng/ml basic

fibroblast growth factor, 90 µg/ml heparin, and 1% penicillin-streptomycin in an incubator at 37°C and 5% CO_2. Medium was changed regularly every 2-3 days and cells were subcultured at ~80% confluence according to manufacturer's protocol. Cells were collected via trypsinization, centrifuged at 200 g for 5 min and resuspended in fresh media at the appropriate concentration for bioreactor addition. The bioreactors used in this study were sterile 50 ml bio-reaction tubes (CELLTREAT, Pepperell, MA) with a hydrophobic membrane cap facilitating the diffusion oxygen and CO_2 into the bioreactors. Bioreactors were not tissue culture treated such that cells would not attach to the surface of the tube. Cells were seeded at a constant cell density of 20,000 cell/cm^2 in bioreactor samples as well as T-75 control flasks. Microparticles were sterilized by UV for 15 minutes before commencing cell attachment. The cell-particle mixture was stirred continuously at 50 rpm in an incubator at 37°C and 5% CO_2 for 24h, thereafter cells were no longer subject to stirring. At 4, 8, and 24h after initial seeding, particles were aspirated from their bioreactors and investigated for cell viability, proliferation, and cell loading capacity. Additionally, control flasks were trypsinized, collected, and subject to the same analysis. Cell viability was determined by staining cells with calcein-AM (CAM) and bright field microscopy. Cell proliferation was determined by performing flow cytometry analysis in conjunction with a live cell assay using CAM staining. Briefly, 200 µl of each bioreactor sample and control was aspirated and collected in 0.6 ml microcentrifuge tubes. CAM was added to each sample at a concentration of 2 µM, and incubated at room temperature for 30 minutes. Subsequently, samples were analyzed using a flow cytometer (BD Accuri C6 Plus, BD Biosciences). Gates were determined for each control (particles, cells, media) and data was analyzed to determine cell concentration, density, and

attachment efficiency. Further, cells-particle samples were fixed with 4%

paraformaldehyde and analyzed by SEM. Additionally, fixed samples were perforated

with 0.1% v/v Triton X-100 in PBS and stained with 30 µl of 5 mg/ml 4',6-diamidino-2-

phenylindole (DAPI) for 5 minutes as well as 205 µl of 6.6 µM tetramethylrhodamine

isothiocyanate (TRITC, rhodamine phalloidin) for 30 minutes. Samples were washed

with PBS, mounted, and dried under vacuum desiccation and subsequently visualized

using confocal laser microscopy (TCS SP8, Leica Camera AG).

3. RESULTS & DISCUSSION

3.1 PARTICLE CHARACTERIZATION

Microparticles in this study were designed to reach a peak size in which the particles would reach a maximum surface area while not sacrificing cell binding ability. Initially, 10% w/v PVA was used as the concentration for particle formulation, however, these microparticles never surpassed 40 μm in diameter. We attempted to alleviate this issue by decreasing the PVA concentration from 10% w/v to 1% w/v, which is known to increase particle size [3], as well as reducing the stirring time of particles after pumping the carrier and organic streams through the flow-focusing device. This resulted in a particle size increase of bare PLGA particles to 122 ± 40.4 μm (Table 1). The bare particles were spherical in shape and displayed a relatively uniform size for larger particles (Figure 1). SEM images indicate that the bare particles are indeed spherical and slightly porous, which is most likely due to evaporation of ethyl acetate prior to washing and evaporation of entrapped water during lyophilization. Zeta potential measurement of the bare PLGA particles was -26.9 mV and -16.7 mV in H_2O and PBS, respectively. These values are lower in absolute value than those typically reported for PLGA [25, 26] which is most likely due to the extreme size of the microparticles which decreases the surface charge density. Modifying the surface of polymeric particles, especially with extracellular matrix constituents or polycationic materials, is known to induce many alterations in the particles' properties [2, 14, 19]. During the coating procedure, particles are coated in a 37°C environment in a solution consisting of PBS. These conditions help facilitate coating through physical adsorption by reducing the strength of the polymer's bonds, by bathing the particle in conditions closer to its glass transition temperature. This causes the

particle to associate with the proteins in solution by increasing the frequency at which

end groups experience van der Waals interactions which induces adhesion of the protein

molecule to the particle surface [27]. Additionally, this elevated temperature catalyzes

degradation of PLGA particles due to hydrolysis [9]. As of a result of these phenomena,

coated particles developed interesting architecture (Figure 1). The brightfield images of

each coated particle, whether gelatin, PLL, or a combination of the two was used as

coating, display a central section surrounded by a lighter area. This result suggests a few

things about these particles. One, that the particles are coated in a relatively thin protein

coating, causing an expansion in particle size (Table 1). Secondly, the particles most

likely have undergone some level of degradation during the 1.5 hr incubation period at

elevated temperature. Comparing the brightfield images (column A, Figure 1) of the

PLGA particles compared to PG, P2, and P2G, the PLGA particles are black and devoid

of light passing through whereas the coated particles are substantially lighter indicating

that more light passing through the aperture and a less dense particle. Additionally,

coated particles are much less regular in shape when compared to the bare PLGA

particles, indicating that protein coating induces shape change in the particles. Comparing

the SEM images in columns B, C, and D, the bare PLGA particles are more regular in

shape and lack the degree of particle debris/degradation in the coated formulations. Most

notable from column B, the act of rotating particles in an elevated temperature

environment seems to induce particle deformation and breaking which is not seen in bare

PLGA particles which are not subject to such forces. PLL coated PLGA particles

especially experience this sort of degradation because much of the particles have

fragmented into irregularly shaped chunks.

Table 1: Particle Characteristics. Average particle diameter is the mean value of 50 or more particles.

Particle Type	Average Particle Diameter	No. of Particles/g	No. of Particles/ml
PLGA	122 ± 40.4 μm	$1.05 \cdot 10^6 \pm 0.193 \cdot 10^6$	3,700
PLGA-Gel	136 ± 42.1 μm	$0.760 \cdot 10^6 \pm 0.122 \cdot 10^6$	3,000
PLGA-PLL	156 ± 39.9 μm	$0.503 \cdot 10^6 \pm 0.133 \cdot 10^6$	2,200
PLGA-PLL/Gel	140 ± 47.0 μm	$0.696 \cdot 10^6 \pm 0.087 \cdot 10^6$	2,800
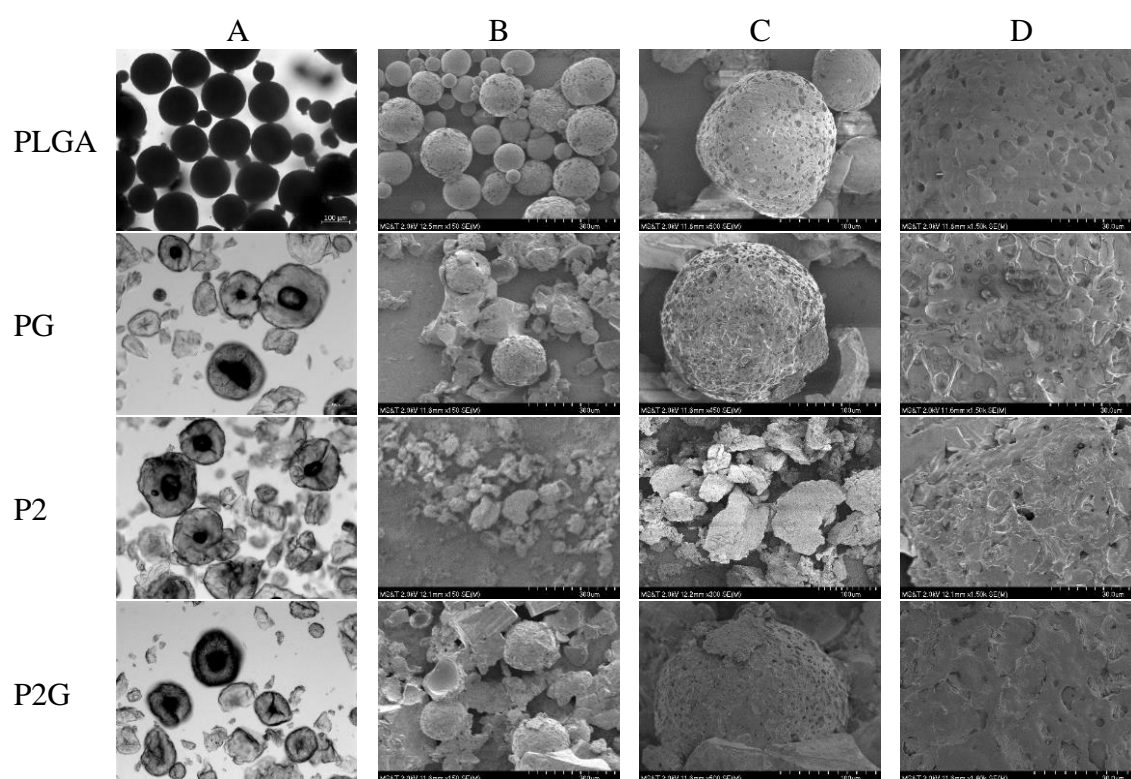
Figure 1: Microscope Images of Particles. (A) Light microscopic images of PLGA microparticles with and without adsorbed coating (10x); SEM images of each particle formulation at (B) 150x, (C) 500x, (D) 1,500x magnifications; (B, C) depict particle morphology, indicating porous structures and a rough surface for protein coated particles; (D) Single particle surface image comparing the roughness and porosity of each particle formulation. Coated particle (PG, P2, P2G) surfaces are rough and irregular indicating a coating has formed on the particle whereas PLGA particles are homogeneous and porous indicating a lack of such coating.   PG = PLGA-Gel; P2 = PLGA-PLL; P2G = PLGA-PLL/Gel

Finally, it is quite apparent that physical adsorption of proteins to microparticles increases the surface roughness of the particles (column D). Particles coated with gelatin and PLL experienced a substantial size increase (Table 1). Size measurement was a crucial part of our investigation because cells were seeded at a constant density based on surface area. Due to the diameter increasing by the protein coating, coated particles had a larger surface area per particle. Thus, less of these particles were necessary to achieve the control area used in cell experiments.

One of the notable changes when modifying microparticle surfaces is the zeta potential measurement. Zeta potential describes the electric potential between a particle surface and the suspension medium at the plane in which counter-ions to the particle surface do not move with the particle [28, 29]. All particles were measured for zeta potential in H_2O and PBS. PBS was used to mimic *in vivo* conditions such as pH and ion concentration. For all coated particles, zeta potential increased in absolute value, whether in H_2O or PBS, compared to bare PLGA particles (Figure 2). Zeta potential values were -27.9, -35.1, and -26.1 mV in H_2O, and -23.4, -25.1, and -19.9 mV in PBS for PG, P2, and P2G respectively. Interestingly, particles coated with PLL (P2) experienced the most negative zeta potential value, which is unusual for PLL coated materials [11, 30]. The zeta potential of gelatin coated particles was negative and higher than that measured for bare PLGA as well. When placed in PBS, all particles had a decrease in zeta potential, relative to when H_2O is the suspension medium. This suggests that coating with proteins like gelatin and amino acid polymers like PLL increases the stability of PLGA microparticles, since a higher absolute value of zeta potential prevents particle aggregation and flocculation [31]. The PLL loading of P2 particles was 6.86 µg/mg

particles which is sufficiently low, given the extreme size of the particles, to prevent a

positive zeta potential. Thus, the loading of coating solution on PLL conjugated particles

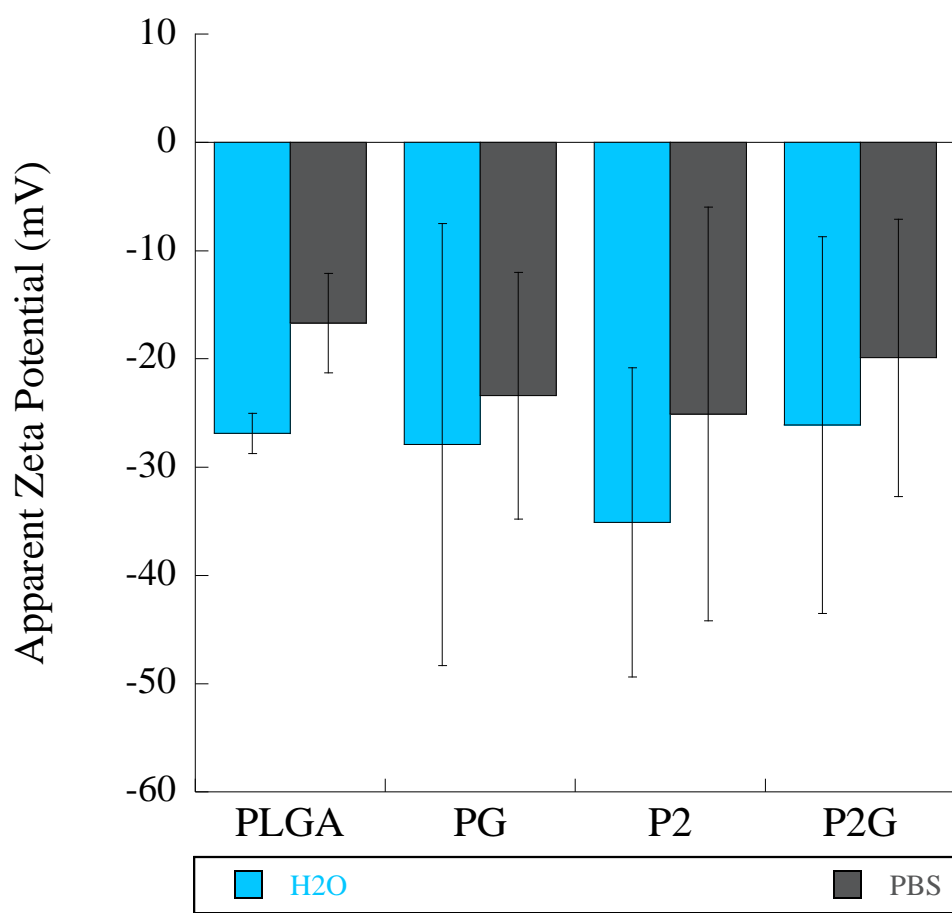is too low to completely cover the surface of the microparticles.

Figure 2: Zeta Potential
Zeta potential for each particle formulation measured by dynamic light scattering (DLS)
and electrophoretic mobility. Each sample was measured in both RO H_2O and PBS, blue
and grey bars, respectively. Error bars are mean ± standard deviation.

3.2 SURFACE MODIFICATION

Particles fabricated from PLGA typically repel cells because of the hydro

hydrophobic nature of the polymer [14, 32, 33], unless the particle surface is modified.

To improve interactions between particles and cells, PLGA microparticles were coated in

PLL, gelatin, or a mixture of both, and analyzed quantitatively using nuclear magnetic

resonance (Table 2). Particles coated with gelatin, PG and P2G, experienced the highest

total conjugation efficiency at 62.9% ± 4.53% and 76.8% ± 4.94%, respectively, while a

conjugation efficiency of 30.6% ± 4.94% was observed for PLL coated particles. Given

the conjugation efficiency, P2G particles, which are a 40/60 mix of PLL/Gelatin, had the

highest coating density and therefore the most protein/poly-amino acid adsorbed. Thus,

there must exist a synergistic adsorption effect for PLL and gelatin on the surface of

PLGA microparticles which may translate to mixtures of proteins other than gelatin.

Table 2: Adsorption Capacity of Microparticles. Particles were loaded with a uniform
ratio of total protein mass to particle mass. P2G particles were prepared using a 60/40
mixture of gelatin/PLL. Conjugation efficiency and protein density was determined using
a standard curve prepared by NMR analysis. Protein density was calculated using the
surface area per mg of bare PLGA particles.

Particle	Initial MassLoading (µg/mg Particles)	Total Conjugation Efficiency	Coating Density (µg/cm^2 Particle)	Adsorbed Coating (µg/mg particles)
PG	6.86	62.9 ± 4.53%	9.79 ± 0.72	4.19 ± 0.310
P2	6.86	30.6 ± 1.51%	4.85 ± 0.194	2.08 ± 0.083
P2G	6.86	76.8 ± 4.94%	12.0 ± 0.79	5.13 ± 0.338

3.3 CELL ATTACHMENT, PROLIFERATION, AND QUANTIFICATION

Particles were prepared using a basis surface area of 14 cm^2 and cells were seeded at a constant cell density of 35,000 cells/cm^2 for both controls and particle samples. Microscope images and flow cytometer measurements were taken at 0, 4 (Figure 3) and 8h (Figure A.1).

Control	PLGA	PG	P2	P2G
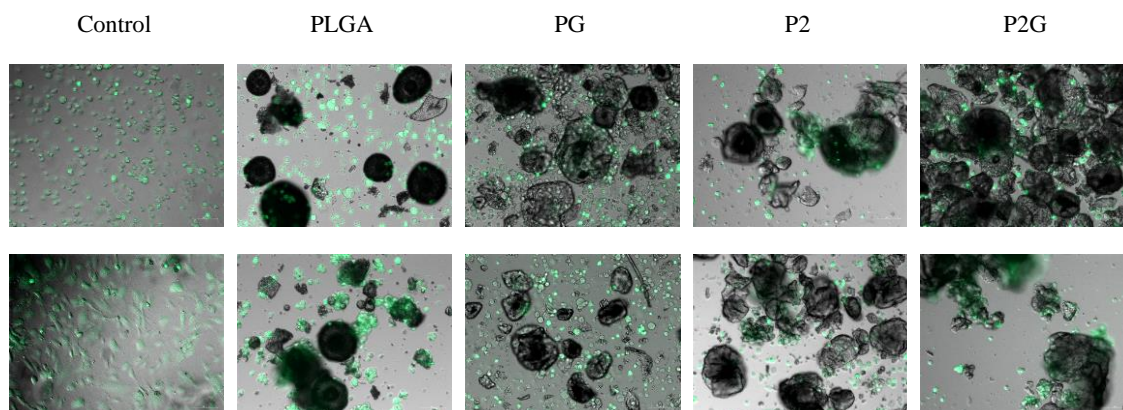
Figure 3: Microscopic Characterization of Cell-laden Particles.
Fluorescent microscope images of cell-particle samples. Top row is images taken at 0h, or initial seeding, and bottom row is images taken at 4h post-seeding. Control images were taken in a 96 well plate, particle samples were aspirated from bioreactor tubes, stained with 2µM CAM, and plated on microscope slides.

Images taken at 0h show viable cells fluorescing green, however, most cells are rounded and not clearly associated with particles, indicating attachment has not occurred. At 4h, cells attach to PLGA particles, but are clustered in aggregates indicating a higher affinity for cell-cell interactions rather than cell-particle binding. However, coated particle samples do not display clear cell aggregation. Cells attached strongly to P2 and P2G particles at four hours whereas PLGA and PG particles show some cell attachment mixed with cell aggregates, with many cells in the fluid surrounding the particles. This

suggests that while cells are present in the samples they do not bind as well to bare PLGA
and gelatin coated PLGA particles.

Cell attachment to particles was further confirmed using confocal laser microscopy
coupled with actin and nucleic staining (Figure 4). Cells were not observed in PLGA
particles, however, PLGA particles physically adsorbed the phalloidin stain giving off a
bright red fluorescence. Surface modified particles, PG, P2, and P2G, all were positive
for cell attachment as confirmed by phalloidin and DAPI fluorescence on the surface of
particles.
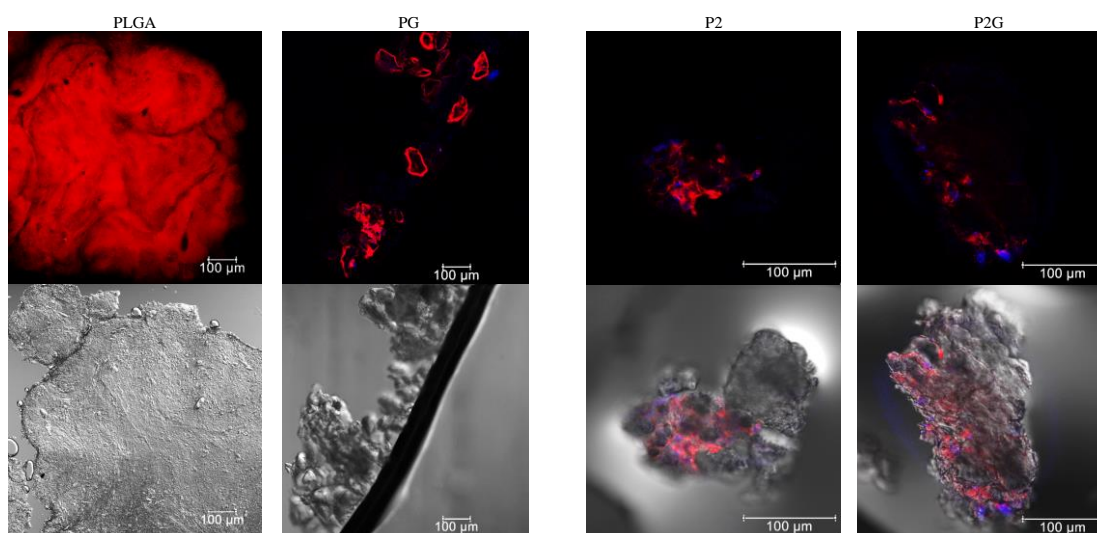
Figure 4: Confocal Laser Microscopy. Microscopic images taken at 20x on a Leica TCS
SP8 confocal laser microscope. (A) PLGA and PG particles, top row: DsRed and DAPI
channels showing actin and nucleic staining; bottom row: light microscopic image of the
same frame. PLGA particles showed no cells in the sample, but adsorbed phalloidin dye.
(B) P2 and P2G particles, top row: DsRed and DAPI channels; bottow row: DsRed,
DAPI, and light channels of particles.

All surface modified particles displayed extensive cell attachment on the edges of the
particle. The extent of cell spreading and attachment on surface modified particles is

confirmed through fluorescent microscopy (Figure 5). Images represent three-dimensional renderings of z-stack compiled images. Cells were stained with calcein AM (CAM). The bottom row resembles a "heat map" of the fluorescent channel depicting the elevation of cells within the 3D rendering confirming that cells have attached and spread on the surface of the particles on the z-axis, or vertical direction.

P2   P2G

Figure 5: Characterization of Cells on Microparticles.
3D rendering of P2 and P2G samples. From top: light microscopy 3D rendering, fluorescent channel 3D rendering, combined 3D rendering, fluorescent channel rendering with elevation gradient. Cells are shown as spreading along the edge of particles on the z-axis confirming that cells have attached and begun to spread.

Cell-particle mixtures were analyzed using flow cytometry to quantify the extent of cell attachment to particles (Figure 6). SSC vs FSC plots resemble the shape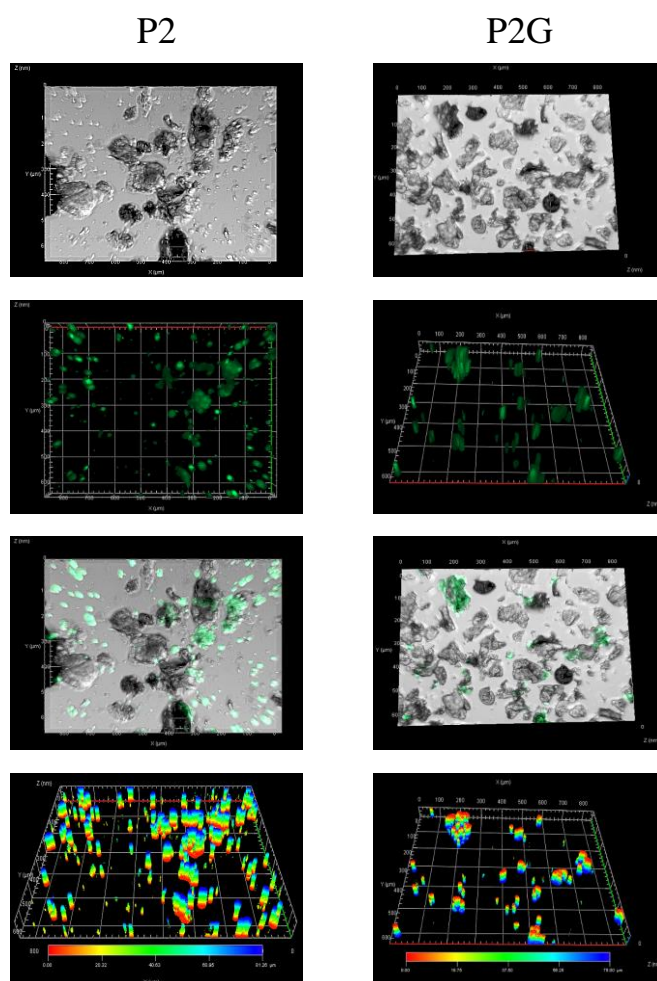 and size of the particles and cells giving an indication to the difference in diameter as well as granularity of the samples. The FSC value indicates how much of the laser passes around the sample while the SSC value indicates how much of the laser beam is reflected off organelles and particulates in the cell and the matrix composing the core of the particles. Dot plots from flow cytometer are colored green for HUVECs and purple for particles (Figure 6a). PLGA, PG, and P2 particles all have a higher SSC value than cells, however, P2G samples are overlapped with HUVECs in the sample. This indicates that cells are strongly bound to P2G particles. The larger SSC value means that the particles reflect more laser than the cells suggesting that particles have a solid core whereas HUVECs have more empty space in their interior. Considering that cells, whether eukaryotic or prokaryotic, are composed of cytoplasm – a gel-like substance – and polymer microparticles are composed of a tight network of polymeric chains, it makes sense that SSC values are higher for microparticles as more of the laser should pass through the cell's translucent cytoplasm.

Flow cytometry data was further analyzed to assess the proliferative capacity of HUVECs bound to microparticles (Figure 6b, c). Cell populations were separated from particles using gates as shown in panel A of Figure 4. The data was correlated for change in cell density, expressed as cell/cm^2, over 8 hours. All samples were initially seeded at 20,000 cells/cm^2 at 0h. Notably, P2G particles realized the largest increase in cell density at 4 hours, whereas PLGA and P2 decreased slightly and control and PG particles experienced a slight increase. At 8 hours, only PG particles increased while all other

particles formulations experienced a significant drop in cell density and control samples were virtually constant.

Figure 6: Cell Proliferation and Quantification.
(A) Flow Cytometry Analysis. Qualitative flow cytometry data for cells mixed with particles at 4h. Dot plots are color labelled as purple = particles; green = cells; M3 = Percentage of samples that are not cells SSC vs FSC graphs depict granularity, or surface roughness, compared to size of the sample. Particles consistently report a higher degree of granularity as well as a bigger size. FITC Count data shows number of events which report a certain fluorescence value – cells stained with CAM report higher values while particles report low values. However, some overlap is observed, especially in PG and P2G which indicates cells and particles are closely associated. SSC vs FITC data aids in determining the extent at which particles and cells are associated. (B) Cell density over time; (C) Relative cell density compared to control at each time point. Cell density estimation determined from flow cytometer data.
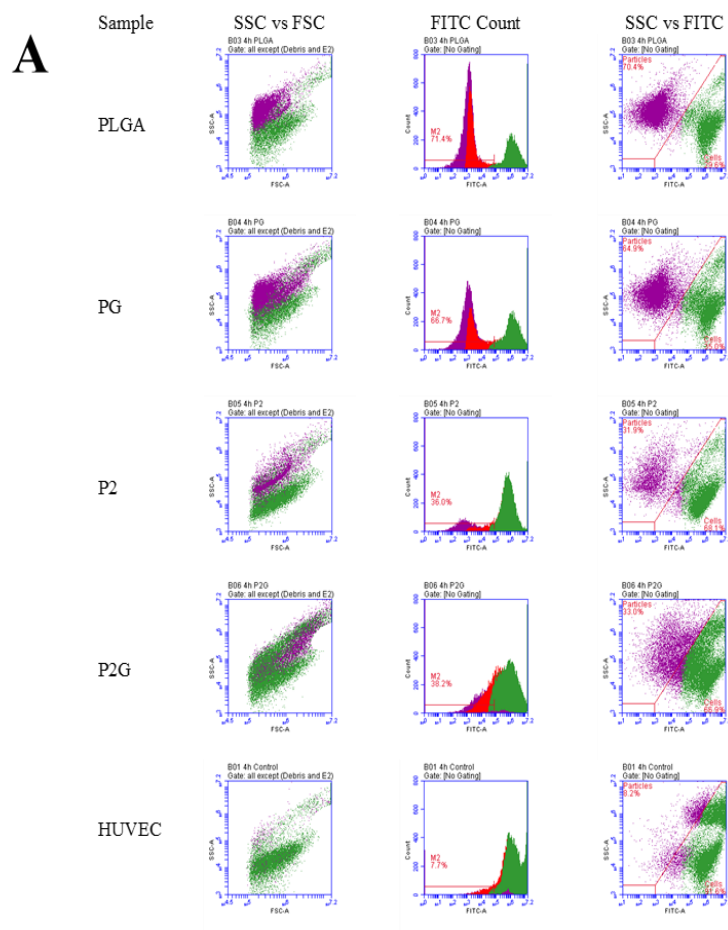
Figure 6: Cell Proliferation and Quantification.
(A) Flow Cytometry Analysis. Qualitative flow cytometry data for cells mixed with particles at 4h. Dot plots are color labelled as purple = particles; green = cells; M3 = Percentage of samples that are not cells SSC vs FSC graphs depict granularity, or surface roughness, compared to size of the sample. Particles consistently report more granularity as well as a bigger size. FITC Count data shows number of events which report a certain fluorescence value – cells stained with CAM report higher values while particles report low values. However, some overlap is observed, especially in PG and P2G which indicates cells and particles are closely associated. SSC vs FITC data aids in determining the extent at which particles and cells are associated. (B) Cell density over time; (C) Relative cell density compared to control at each time point. Cell density estimation determined from flow cytometer data.

3.4 DISCUSSION

Endothelial cells are integral to maintaining homeostasis and repairing severely damaged tissues. They are responsible for lining blood vessels which deliver nutrients and oxygen, both critical components of cellular health and function – especially in tissue repair processes – as well as transport waste to the excretory system. Endothelial cells act as a barrier between the lumen of blood vessels, where erythrocytes are located, to the surrounding tissues by mediating the passage of white blood cells and other materials. Due to their extensive presence in the body – endothelial cells are found throughout the

entire circulatory system – endothelial cells have been investigated for their potential in tissue engineering [34]. However, much of the literature has not focused on endothelial cell delivery in tissue engineering, especially when using microparticles as a scaffold. Microparticles offer a unique solution for the regeneration of tissues as they are easily transportable and applied to virtually any tissue. Delivering cells *via* microparticles will provide a versatile vehicle for augmenting the regeneration of tissues. Additionally, modelling the microparticle system with HUVECs will produce a universal system for attachment of most any cell line.

To investigate the capability of PLGA microparticles as a cell delivery vehicle of HUVECs, particles were fabricated at a size of more than 100 µm and coated with PLL, a cationic polymer, gelatin, a remnant of the extracellular matrix protein collagen, or a combination of both. HUVECs were cultured with microparticles in non-treated bioreactors for a facile and portable approach to attaching cells to a scaffold. Interestingly, a combination of both PLL and gelatin yielded the most cell attachment to particles, compared to bare and separately coated particles. Cationic polymers [35], like PLL, are known to induce cell association with coated surfaces through cationic interactions [36]. The plasma membrane surrounding cells is typically negatively charged, while PLL is positively charged due to the ε-ammonium group on the lysine side chain [37]. The cationic nature of PLL attracts cells at the plasma membrane *viz* electrostatic forces [38], the extent of which is pH dependent [39, 40]. Thus, coating the surface of biomaterials with PLL causes more cells to attach and proliferate [8]. After attachment, cells typically spread on a surface and use special protein domains to anchor themselves. However, PLL only participates in non-specific cationic adherence of cells

[38] whereas other molecules bind cells through integrins [41, 42]. Integrins are a class of transmembrane proteins that bind cells using cell-recognition motifs [43]. The motifs are comprised of specific amino acid sequences like RGD [44] in fibronectin and YIGSR in laminin [12, 46]. When integrins bind to these motifs the cell undergoes phenotypic changes that cause anchoring and spreading on the surface. Gelatin is believed it act on these integrin receptors as it is a derivative of collagen, an extracellular matrix protein which anchors cells together, however, since gelatin is in a degraded form it is not as effective and most likely has a lower concentration of integrin binding sequences. Quirk et al. demonstrated the effect of differing concentrations of PLL conjugated to GRGDS, a cell-recognition motif, on the extent of cell spreading using poly-lactic acid films. Conjugating PLL to GRGDS resulted in improved spreading of cells and was comparable to cells grown in tissue culture plates [22]. Plasma polymerization is another technique to functionalize the surface of scaffolds for cell attachment [5, 23, 24, 47, 48]. Plasma polymerization requires special machinery to apply a plasma gas coating to the scaffold, which increases fabrication cost. Allyl amine is a typical compound for plasma surface treatment of bioactive scaffolds to increase cell binding. Bible et al. demonstrated that plasma deposition of allyl amine on the surface of PLGA particles improved cell attachment to microparticles compared to a coating of only fibronectin or PLL [24]. However, this process requires a plasma reactor capable of gasifying a compound and subsequently depositing it on the surface of a scaffold, which typically requires a propriety device developed *in situ*.

Interestingly, PG particles only coated with gelatin did not bind cells well compared to other particle formulations (Figure 3). Considering gelatin is a derivative of collagen,

there should be some remnants of integrin binding domains in its amino acid configuration. However, PG particles had a negative zeta potential (Figure 2), thus indicating that the surface of these particles carries a negative charge. The plasma membrane of cells also carries a negative charge, and consequently should repel the surface of the PG particles. P2G particles, which are coated in both PLL and gelatin, attached cells very well, most likely due to the cationic charge of PLL attracting cells and the amino acid sequencing of gelatin enabling anchoring and spreading of cells once they are in proximity to the particle surface. P2 particles, coated only with PLL, also saw distinct cell association with the particle surface, however, PLL is known to be cytotoxic [22, 37, 49]. In a parallel investigation, we studied the ability for PLL to attach MDA-MB-231 breast cancer cells over 7 days (Figure A.2). These cancer cells lost viability after 3 days in culture in PLL only coated particles, suggesting that the use of only PLL is not suitable for cellular attachment on scaffolds meant for tissue engineering.

Microparticles can fabricated as spheres, disks, and rods [50]. In this investigation, only spheres were analyzed for cell binding potential, however, rods have the advantage of maintaining the same surface area as a sphere but having a more intense curvature. Cells like to associate with surfaces that have intense curvature as this aids in spreading as well as mimics the environment present in the body. Additionally, only HUVECs were investigated for binding potential. Each cell line will have unique results when assessed for binding potential to PLGA particles. Each tissue in the human body has its own spectrum of cells each with different concentrations of integrins as well as varying composition of these integrin proteins which effect their binding potential to bioactive scaffolds. To account for these variations, particles can be modified with different

extracellular matrix constituents or various cationic polymers to optimize attachment of each cell type. PLGA particles can be copolymerized with other functional polymers such as polyethylene glycol (PEG) [6, 32, 51] or polyethylene imine (PEI) [35] to aid in cell association for delivery to tissues *in vivo*.

Further analysis is necessary to assess the potential of these microparticles cultured with cells to regenerate tissue. *In vivo* or *ex vivo* studies should be conducted to assess therapeutic potential of PLGA microparticles to remediate blood vessel damage as well as induce vascularization and angiogenesis in ischemic tissues. Additionally, particles should be fabricated as different shapes, such as rods and disks, to assess the optimum shape for cell attachment. Other cell lines should be investigated and compared quantitatively to determine the extent at which these particles can bind a range of cell lines as well as gain insight into the binding domains across various cells. Lastly, modifying the microparticle surface with various extracellular matrix proteins and cationic polymers and assessing their binding affinities for cells, especially HUVECs, would aid in optimizing particle formulation for maximum tissue recovery.

4. CONCLUSION

In summary, PLGA microparticles functionalized with PLL and gelatin successfully attached HUVEC cells, maintained cell viability, and enabled proliferation. This proves that a simple fabrication method (Figure A.3) of microparticles coupled with facile physical adsorption is capable of effectively binding cells for therapeutic use as well as manufacturing large particles with sizable control. This study demonstrates that HUVEC cells can be bound to microparticles without the use of complicated machinery, like plasma polymerization, and surface modification requiring expensive materials, such as purified and sterilized fibronectin or laminin. These results can be further illustrated by applying these microparticles cultured with HUVEC cells to mice models and assessing their potential for therapeutic recovery of ischemic tissues.

In addition to physical adsorption for protein coating, chemical conjugation was investigated as a method to modify particles with protein, like gelatin. The bicinchoninic acid (BCA) assay is a quick and versatile tool for quantifying protein, like fibronectin, collagen, or gelatin, in a sample. This quantification is important data because accurate analysis of total protein adsorbed or chemically bound to a particle provides an interpretation into how cells respond to certain concentrations of protein. Too much or too little adsorbed protein can drastically change cell phenotype leading to unhealthy cells. Additionally, theoretical modelling and simulation of cell signaling mechanisms requires precise and accurate data to be valid. Thus, paper II describes a method for correcting N-hydroxysuccinimide (NHS) in the BCA assay.

REFERENCES

[1] W. Jiang, R. K. Gupta, M. C. Deshpande, and S. P. Schwendeman, "Biodegradable poly(lactic-co-glycolic acid) microparticles for injectable delivery of vaccine antigens," *Adv Drug Deliv Rev,* vol. 57, pp. 391-410, Jan 10 2005.

[2] M. J. Tsung and D. J. Burgess, "Preparation and characterization of gelatin surface modified PLGA microspheres," *PharmSci,* vol. 3, p. No pp. given, // 2001.

[3] S. K. Sahoo, A. K. Panda, and V. Labhasetwar, "Characterization of Porous PLGA/PLA Microparticles as a Scaffold for Three Dimensional Growth of Breast Cancer Cells," *Biomacromolecules,* vol. 6, pp. 1132-1139, // 2005.

[4] Z. Ding, J. Chen, S. Gao, J. Chang, J. Zhang, and E. T. Kang, "Immobilization of chitosan onto poly-l-lactic acid film surface by plasma graft polymerization to control the morphology of fibroblast and liver cells," *Biomaterials,* vol. 25, pp. 1059-1067, 2004/03/01/ 2004.

[5] J. H. Zhao, J. Wang, M. Tu, B. H. Luo, and C. R. Zhou, "Improving the cell affinity of a poly(D,L-lactide) film modified by grafting collagen via a plasma technique," *Biomed Mater,* vol. 1, pp. 247-52, Dec 2006.

[6] U. Wattendorf and H. P. Merkle, "PEGylation as a tool for the biomedical engineering of surface modified microparticles," *J Pharm Sci,* vol. 97, pp. 4655-69, Nov 2008.

[7] H. M. Mansour, M. Sohn, A. Al-Ghananeem, and P. P. Deluca, "Materials for pharmaceutical dosage forms: molecular pharmaceutics and controlled release drug delivery aspects," *Int J Mol Sci,* vol. 11, pp. 3298-322, Sep 15 2010.

[8] I. P. Monteiro, A. Shukla, A. P. Marques, R. L. Reis, and P. T. Hammond, "Spray-assisted layer-by-layer assembly on hyaluronic acid scaffolds for skin tissue engineering," *J Biomed Mater Res A,* vol. 103, pp. 330-40, Jan 2015.

[9] O. I. C. M. Dunne, Z. Ramtoola, "Influence of particle size and dissolution conditions on the degradaiton properties of PLGA," *Biomaterials,* vol. 21, pp. 1659-1668, 2000.

[10] J. Yu, A.-R. Lee, W.-H. Lin, C.-W. Lin, Y.-K. Wu, and W.-B. Tsai, "Electrospun PLGA Fibers Incorporated with Functionalized Biomolecules for Cardiac Tissue Engineering," *Tissue Engineering. Part A,* vol. 20, pp. 1896-1907, 06/10

[11] G. J. Delcroix, E. Garbayo, L. Sindji, O. Thomas, C. Vanpouille-Box, P. C. Schiller*, et al.*, "The therapeutic potential of human multipotent mesenchymal stromal cells combined with pharmacologically active microcarriers transplanted in hemi-parkinsonian rats," *Biomaterials,* vol. 32, pp. 1560-73, Feb 2011.

[12]   K. D. Newman and M. W. McBurney, "Poly(D,L lactic-co-glycolic acid) microspheres as biodegradable microcarriers for pluripotent stem cells," *Biomaterials,* vol. 25, pp. 5763-71, Nov 2004.

[13]   S. Poilil Surendran, R. George Thomas, M. J. Moon, and Y. Y. Jeong, "Nanoparticles for the treatment of liver fibrosis," *International Journal of Nanomedicine,* vol. 12, pp. 6997-7006, 09/20 2017.

[14]   H. Tan, D. Huang, L. Lao, and C. Gao, "RGD modified PLGA/gelatin microspheres as microcarriers for chondrocyte delivery," *J Biomed Mater Res B Appl Biomater,* vol. 91, pp. 228-38, Oct 2009.

[15]   H. Chen, Y. Peng, S. Wu, and L. P. Tan, "Electrospun 3D Fibrous Scaffolds for Chronic Wound Repair," *Materials (Basel),* vol. 9, Apr 6 2016.

[16]   J. M. Anderson and M. S. Shive, "Biodegradation and biocompatibility of PLA and PLGA microspheres," *Advanced Drug Delivery Reviews,* vol. 64, pp. 72-82, 2012.

[17]   r. W. Stroncek JD, *Overview of Wound Healing in Different Tissue Types*. Boca Raton (FL): CRC Press/Taylor & Francis, 2008.

[18]   A. M. Pereira, R. Machado, A. da Costa, A. Ribeiro, T. Collins, A. C. Gomes*, et al.*, "Silk-based biomaterials functionalized with fibronectin type II promotes cell adhesion," *Acta Biomaterialia,* vol. 47, pp. 50-59, 2017/01/01/ 2017.

[19]   J.-E. Lee, J.-C. Park, Kwang H. Lee, Sang H. Oh, and H. Suh, "Laminin Modified Infection-Preventing Collagen Membrane Containing Silver Sulfadiazine– Hyaluronan Microparticles," *Artificial Organs,* vol. 26, pp. 521-528, 2002.

[20]   L. Lao, H. Tan, Y. Wang, and C. Gao, "Chitosan modified poly(L-lactide) microspheres as cell microcarriers for cartilage tissue engineering," *Colloids Surf B Biointerfaces,* vol. 66, pp. 218-25, Oct 15 2008.

[21]   S. Barua, J. Ramos, T. Potta, D. Taylor, H.-C. Huang, G. Montanez*, et al.*, "Discovery of Cationic Polymers for Non-viral Gene Delivery using Combinatorial Approaches," *Combinatorial chemistry & high throughput screening,* vol. 14, pp. 908-924, 2011

[22]   R. A. Quirk, W. C. Chan, M. C. Davies, S. J. B. Tendler, and K. M. Shakesheff, "Poly(l-lysine)–GRGDS as a biomimetic surface modifier for poly(lactic acid)," *Biomaterials,* vol. 22, pp. 865-872, 2001/04/01/ 2001.

[23]   J. Yang, J. Bei, and S. Wang, "Enhanced cell affinity of poly (d,l-lactide) by combining plasma treatment with collagen anchorage," *Biomaterials,* vol. 23, pp. 2607-2614, // 2002.

[24]   E. Bible, D. Y. S. Chau, M. R. Alexander, J. Price, K. M. Shakesheff, and M. Modo, "Attachment of stem cells to scaffold particles for intra-cerebral transplantation," *Nat. Protocols,* vol. 4, pp. 1440-1453, 09//print 2009.

[25] L. Chronopoulou, M. Massimi, M. F. Giardi, C. Cametti, L. C. Devirgiliis, M. Dentini*, et al.*, "Chitosan-coated PLGA nanoparticles: a sustained drug release strategy for cell cultures," *Colloids Surf B Biointerfaces,* vol. 103, pp. 310-7, Mar 01 2013.

[26] Y. P. Li, Y. Y. Pei, X. Y. Zhang, Z. H. Gu, Z. H. Zhou, W. F. Yuan*, et al.*, "PEGylated PLGA nanoparticles as protein carriers: synthesis, preparation and biodistribution in rats," *J. Controlled Release,* vol. 71, pp. 203-211, // 2001.

[27] J. Tao and A. M. Rappe, "Physical adsorption: theory of van der Waals interactions between particles and clean surfaces," *Phys Rev Lett,* vol. 112, p. 106101, Mar 14 2014.

[28] D. Hanaor, M. Michelazzi, C. Leonelli, and C. C. Sorrell, "The effects of carboxylic acids on the aqueous dispersion and electrophoretic deposition of ZrO2," *Journal of the European Ceramic Society,* vol. 32, pp. 235-244, 2012.

[29] R. Chen, S. J. Curran, J. M. Curran, and J. A. Hunt, "The use of poly(l-lactide) and RGD modified microspheres as cell carriers in a flow intermittency bioreactor for tissue engineering cartilage," *Biomaterials,* vol. 27, pp. 4453-60, Sep 2006.

[30] H. Nojehdehian, F. Moztarzadeh, H. Baharvand, H. Nazarian, and M. Tahriri, "Preparation and surface characterization of poly-L-lysine-coated PLGA microsphere scaffolds containing retinoic acid for nerve tissue engineering: in vitro study," *Colloids Surf B Biointerfaces,* vol. 73, pp. 23-9, Oct 1 2009.

[31] P. Sarkar and P. S. Nicholson, "Electrophoretic Deposition (EPD): Mechanisms, Kinetics, and Application to Ceramics," *Journal of the American Ceramic Society,* vol. 79, pp. 1987-2002, 1996.

[32] B. Jeong, K. M. Lee, A. Gutowska, and Y. H. An, "Thermogelling Biodegradable Copolymer Aqueous Solutions for Injectable Protein Delivery and Tissue Engineering," *Biomacromolecules,* vol. 3, pp. 865-868, 2002/07/01 2002.

[33] K. W. Chun, H. S. Yoo, J. J. Yoon, and T. G. Park, "Biodegradable PLGA Microcarriers for Injectable Delivery of Chondrocytes: Effect of Surface Modification on Cell Attachment and Function," *Biotechnology Progress,* vol. 20, pp. 1797-1801, 2004.

[34] C.-C. Huang, W.-Y. Pan, M. T. Tseng, K.-J. Lin, Y.-P. Yang, H.-W. Tsai*, et al.*, "Enhancement of cell adhesion, retention, and survival of HUVEC/cbMSC aggregates that are transplanted in ischemic tissues by concurrent delivery of an antioxidant for therapeutic angiogenesis," *Biomaterials,* vol. 74, pp. 53-63, 2016/01/01/ 2016.

[35] Y. S. Lee, K. S. Lim, J. E. Oh, A. R. Yoon, W. S. Joo, H. S. Kim*, et al.*, "Development of porous PLGA/PEI1.8k biodegradable microspheres for the delivery of mesenchymal stem cells (MSCs)," *J Control Release,* vol. 205, pp. 128-33, May 10 2015.

[36] D. S. Hwang, S. B. Sim, and H. J. Cha, "Cell adhesion biomaterial based on mussel adhesive protein fused with RGD peptide," *Biomaterials,* vol. 28, pp. 4039-46, Oct 2007.

[37] T. B. Project. (2003). *Lysine. The Biology Project, Department of Biochemistry and Molecular Biophysics, University of Arizona*.

[38] B. S. Jacobson and D. Branton, "Plasma membrane: rapid isolation and exposure of the cytoplasmic surface by use of positively charged beads," *Science,* vol. 195, p. 302, 1977.

[39] K. Kono, S. Kimura, and Y. Imanishi, "pH-Dependent interaction of amphiphilic polypeptide poly(Lys-Aib-Leu-Aib) with lipid bilayer membrane," *Biochemistry,* vol. 29, pp. 3631-3637, 1990/04/17 1990.

[40] S. C. Yasui and T. A. Keiderling, "Vibrational circular dichroism of polypeptides. 8. Poly(lysine) conformations as a function of pH in aqueous solution," *Journal of the American Chemical Society,* vol. 108, pp. 5576-5581, 1986/09/01 1986.

[41] E. Ruoslahti, "RGD AND OTHER RECOGNITION SEQUENCES FOR INTEGRINS," *Annual Review of Cell and Developmental Biology,* vol. 12, pp. 697-715, 1996/11/01 1996.

[42] J. L. Guan, J. E. Trevithick, and R. O. Hynes, "Fibronectin/integrin interaction induces tyrosine phosphorylation of a 120-kDa protein," *Cell Regulation,* vol. 2, pp. 951-964, 1991.

[43] M. B. Srichai and R. Zent, "Integrin Structure and Function," pp. 19-41, 2010.

[44] S. Seo and K. Na, "Mesenchymal stem cell-based tissue engineering for chondrogenesis," *J Biomed Biotechnol,* vol. 2011, p. 806891, 2011.

[45] K. D. Newman and M. W. McBurney, "Poly(D,L lactic-co-glycolic acid) microspheres as biodegradable microcarriers for pluripotent stem cells," *Biomaterials,* vol. 25, pp. 5763-71, Nov 2004.

[46] U. Hersel, C. Dahmen, and H. Kessler, "RGD modified polymers: biomaterials for stimulated cell adhesion and beyond," *Biomaterials,* vol. 24, pp. 4385-4415, 2003.

[47] P. K. Chu, J. Y. Chen, L. P. Wang, and N. Huang, "Plasma-surface modification of biomaterials," *Materials Science and Engineering: R: Reports,* vol. 36, pp. 143-206, 2002/03/29/ 2002.

[48] S. Yoshida, K. Hagiwara, T. Hasebe, and A. Hotta, "Surface modification of polymers by plasma treatments for the enhancement of biocompatibility and controlled drug release," *Surface and Coatings Technology,* vol. 233, pp. 99-107, 2013/10/25/ 2013.

[49] I. C. Rawil F Fakhrullin, Yuri Lvov, *Cell Surface Engineering: Fabrication of Functional Nanoshells*. UK: Royal Society of Chemistry, 2014.

[50] S. Barua, J. W. Yoo, P. Kolhar, A. Wakankar, Y. R. Gokarn, and S. Mitragotri, "Particle shape enhances specificity of antibody-displaying nanoparticles," *Proceedings of the National Academy of Sciences of the United States of America,* vol. 110, pp. 3270-3275, Feb 26 2013.

[51] J. Cheng, B. A. Teply, I. Sherifi, J. Sung, G. Luther, F. X. Gu*, et al.*, "Formulation of functionalized PLGA-PEG nanoparticles for in vivo targeted drug delivery," *Biomaterials,* vol. 28, pp. 869-76, Feb 2007.

II.   CORRECTION IN BICINCHONINIC ACID (BCA) ABSORBANCE ASSAY TO ANALYZE PROTEIN CONCENTRATION

ABSTRACT

Conducting the bicinchoninic acid (BCA) assay directly after a coupling reaction using (1-ethyl-3-(3-dimethylaminopropyl) carbodiimide) (EDC) and *N*-hydroxysuccinimide (NHS) chemistry produces significant errors. Here we present a correction for the quantification of gelatin in the supernatant (SN) following gelatin conjugation to polymer microparticles using EDC and NHS chemistry. Following the conjugation reaction, supernatants (SNs) from the gelatin-microparticle formation reaction are treated with BCA assay reagents and quantified for the percentage of unbound gelatin in the solution. NHS was found to interfere with the BCA assay reagents and is dependent on incubation time. It is found that the large concentration (500 µg/ml) of NHS in the conjugation reaction interferes with the sensitivity of gelatin present in SNs. The interference from NHS requires a careful analysis to distinguish the BCA background absorbance from the sample absorbance. Using an NHS control solution can correct NHS interference and thus decrease the expensive iterations in gelatin quantification and enable accurate analysis of gelatin content. The accuracy of gelatin quantification is further improved by reducing the BCA assay incubation time to approximately 20 min, compared to the recommended 30 min. This re-assessment of BCA assay is important to avoid misestimating biases in bioconjugation processes.

1. INTRODUCTION

Bioconjugation is a driving force behind discoveries in life sciences, through the development of new therapeutics, drug targets, and diagnostics [1-4]. One significant impact of bioconjugation chemistry is in the quantification of total protein concentration that serves as a key variable for process development and quality control. The total protein release in the sample supernatant gives an estimate of unbound or secreted proteins during a bioconjugation process. Total protein quantification calls for an accurate, sensitive, robust and cost-efficient method. Despite substantial improvements in commonly used bioassays, quantitative measurements of bioconjugation still face difficulties from unexpected interferences [5-8]. For example, carbodiimide bioconjugations using 1-ethyl-3-(3-(dimethylamino)propyl) carbodiimide (EDC) and *N*-hydroxysuccinimide (NHS) are often used for water-soluble protein bioconjugates with polymeric backbone [9-12]. However, little attention has focused on identifying the quantity of protein being conjugated to the surface of microparticles while unreacted reagents such as EDC and NHS may cause interference during the quantification assay [13-15]. The bicinchoninic acid (BCA) assay is a cost-effective and is highly selective method for determining protein concentrations, which significantly reduces the effect of interfering substances compared to the Lowry or Biuret protein assays [16].

Our findings suggest that when measuring a protein-based polymer material, such as gelatin, both the NHS concentration and incubation time in BCA assay must be reduced from the standard protocol procedure in order to minimize the effect of NHS on the absorbance measurement.

2. MATERIAL & METHODS

2.1 PREPARATION OF GELATIN SUPERNATANT SAMPLES

Gelatin SN Samples used for BCA analysis were prepared from an EDC/NHS

conjugation procedure [17]. EDC/NHS conjugation was used because it is a simple and

effective method to bind a protein to a substrate. The reaction simply reacts a carboxylic

acid (-COOH) group to an amine group ($-NH_2$) forming an amide bond. Briefly, gelatin

from bovine (Sigma-Aldrich) was conjugated to the surface of PLGA and PLGA-PEG

microparticles by coupling primary amines of gelatin with carboxyl groups of PLGA to

form amide bonds (NHS and Sulfo-NHS Instructions, Thermo Scientific). Particles were

suspended at 10 mg/ml in an aqueous activation buffer: 0.1 M 2-

(morpholino)ethanesulfonic acid (MES; Sigma-Aldrich) and 0.5 M NaCl (Fisher

Scientific) with an adjusted pH of 6.0. Activation of carboxyl groups on the PLGA

microparticle surface was accomplished through the successive additions of EDC

(Thermo Scientific) and NHS (Thermo Scientific) to yield an amine-reactive NHS ester.

Final concentrations of EDC and NHS in each reaction mixture were 0.333 mg/ml and

0.5 mg/ml, respectively. After increasing the mixture pH above 7.0, 200 µl of a 0.37%

(w/v) gelatin protein solution was added to the reaction mixtures resulting in 740 µg of

gelatin initially added, which was based on a 1.5:1 protein to particle surface area ratio.

The mixture was shaken (Fisherbrand™ Multi-Platform Shaker, Fisher Scientific) at 450

rpm for 2 h at room temperature. After 2 h, particles were separated by microfiltration

using a 500 µl microcentrifuge filter (Amicon) capable of filtering out 100 kDa

molecules. The device was centrifuged at 14,000 g for 10 min and was used three times

for a total sample volume of 3 ml. This sample was used subsequently in the BCA Assay.

2.2 BCA ASSAY

To determine the protein concentration in SN samples, a modified version of the BCA Assay was used. First, gelatin protein standards were created in PBS to reflect the conditions of SN samples as well as to model the absorbance behavior of the samples. The unknown concentrations of SN samples were prepared in 1 and 50 times dilution. Bovine serum albumin (BSA) of 2000 µg/ml was used as a positive control. Each sample and standard of 25 µl were added to individual wells with three replications in a 96 well plate. A working reagent ratio of 8:1 was used such that 200 µl of BCA working reagent was added to each well. Absorbance was read at 562 nm and 37°C in a microplate reader (Synergy 2) at varying intervals throughout the course of the investigation. The PBS blank was subtracted from the absorbance measurements of all individual standard and unknown samples. A gelatin standard curve was prepared by plotting each gelatin concentration in µg/ml *versus* its average blank-corrected 562 measurements to determine the gelatin concentration of unknown samples.

The absorbance kinetics of varying concentrations of NHS was investigated to compare the kinetics trend of the SN samples to approximate the concentration of NHS in the SN samples. Mixtures of 500, 400, 300, 200, and 100 µg/ml of NHS were prepared in PBS. The NHS samples were prepared in a 96 well plate using the BCA Assay method described previously and absorbance was measured every minute for 2 h at 37°C.

Additionally, gelatin standards were created with EDC and NHS concentrations the same as that used in the conjugation reaction procedure. Data acquired from the BCA protein assay were analyzed to determine protein concentration at each data point. The

data were further processed to determine conjugation percentage of protein, where

conjugation percentage is defined by the following equation:

$$Conjugation\ \% = \frac{Total\ Gelatin - SN\ Gelatin}{Total\ Gelatin} \times 100\% \qquad (2)$$

To calculate protein concentration, all samples were blank (PBS) corrected.

Additionally, SN samples were "NHS corrected" by subtracting the NHS blank that

contained no gelatin (after subtracting the PBS only blank).

2.3 BCA ASSAY CORRECTED BY PRECIPITATION OF GELATIN

To confirm the concentration of gelatin in supernatant samples, a portion of the

supernatant was treated with the Compat-Able Protein Assay kit and subsequently

analyzed with the BCA Assay. Briefly, 50 μl of each supernatant sample were transferred

into a 1.7 ml microcentrifuge tube. Then 500 μl of Compat-Able Protein Reagent 1 was

added and the solution stood undisturbed for 5 min. Next 500 μl of Compat-Able Protein

Reagent 2 was added and the solution was centrifuged at 10,000 g for 10 min. The

resultant supernatant was aspirated and discarded, and the protein pellet was resuspended

in 50 μl of PBS by vortexing and sonication. Additionally, standards containing a known

concentration of gelatin and standards with gelatin and a fixed NHS concentration were

prepared and treated as described above. All samples, after pellet resuspension, were

analyzed using the standard BCA assay protocol.

2.4 STATISTICAL ANALYSIS

Statistical analysis was performed using the Student's t-test by calculating mean and standard deviation with at least three independent experiments. Results were considered significant for p values of < 0.05.

3. RESULTS & DISCUSSION

3.1 NHS CONCENTRATION AFFECTS BCA-BASED GELATIN QUANTIFICATION

To our knowledge, up to now no statistically significant data has been provided in the literature indicating how protein mixed with NHS responds to the BCA working reagent over time. To determine an appropriate NHS concentration and incubation period for measuring the unknown gelatin concentration, a kinetics test was conducted on a variety of controls as well as the unknown SN samples at 30 min intervals between 0 to 2 h (Figure 1). BSA was used as a positive control in conjunction with NHS as a means to correct for NHS interference. As it is seen in Figure 1, BSA (━) has a much stronger absorbance (~3 ± 0.14) than NHS (▷; ~2.25 ± 0.26) or gelatin (○; ~0.95 ± 0.38) that allows BSA to have looser incubation time limits than that of gelatin.
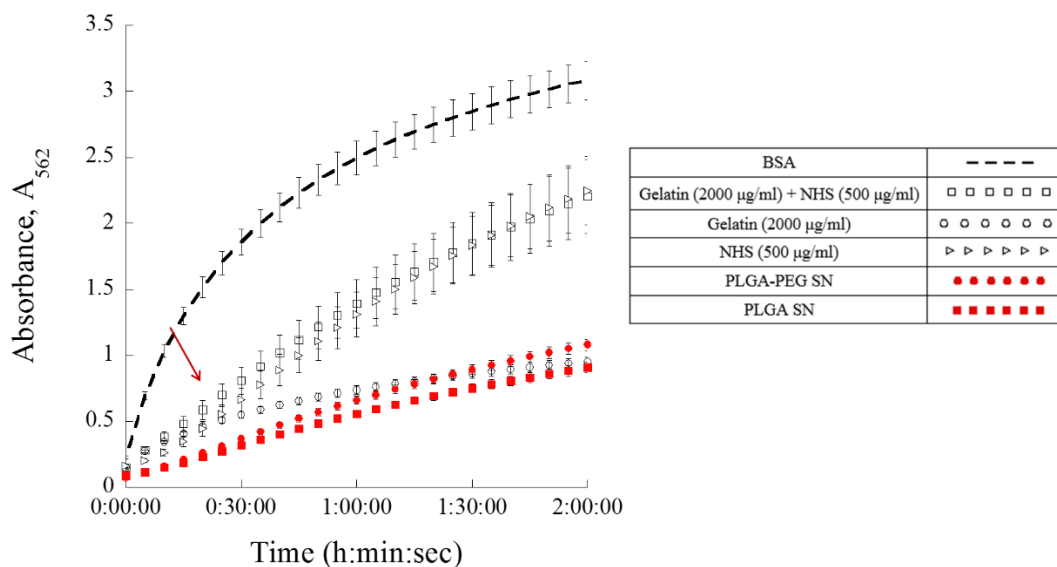

Figure 1: BCA Assay Kinetics. Absorbance rate measurement of bovine serum albumin (BSA) protein, gelatin with NHS, gelatin alone, NHS alone, and sample SNs. Data was taken every 30 seconds for 2 h. Test was conducted at 37°C throughout its entirety. Arrow indicates point of interest at ~20 min where gelatin and NHS responses are equal.

Additionally, BSA has a much steeper absorbance rate than NHS or gelatin, which suggests that BSA may be incubated longer for accurate estimations. This is not the case for gelatin alone and SNs. In fact, the slopes for gelatin alone and SN curves are flatter. The absorbance of NHS surpassed that of only gelatin (arrow), as well as the SNs' absorbance, before 30 min indicating a strong interference from NHS. To test this hypothesis, an additional kinetics study was conducted by varying the concentration (0-500 μg/ml) of NHS to determine the minimum NHS concentration that would eliminate the background noise and whose BCA absorbance is lesser than unknown SNs (Figure 2). Our results suggest that a concentration of 100 μg/ml NHS coincides with the concentration of NHS within the SNs. The SN absorbance is lower than the NHS absorbance until approximately 30 min (Figure 2) suggesting that an accurate correction is dependent on incubation time.

Figure 2: BCA Assay Kinetics of NHS. Data was acquired every 30 s for 2 h and incubated at 37°C for the entire duration. NHS concentrations range from 100-500 μg/ml.

To test the effect of incubation time further, the samples were read for absorbance every minute for 45 min in future experiments. To confirm the impact of NHS concentration again, as well as determine an appropriate incubation time, gelatin standards were prepared with 100 µg NHS/ml and absorbance was measured using the BCA protein assay in addition to the SN samples (Figure 3). The SN samples correlated similarly with the standards and measured above the blank NHS (100 µg/ml of NHS). The incubation time was another contributing factor. SN samples maintained a similar slope to that of the standard prepared at 125 µg/ml gelatin up to 30 min after which it matched with the 250 µg/ml gelatin standard curve. We confirmed this concentration as follows.

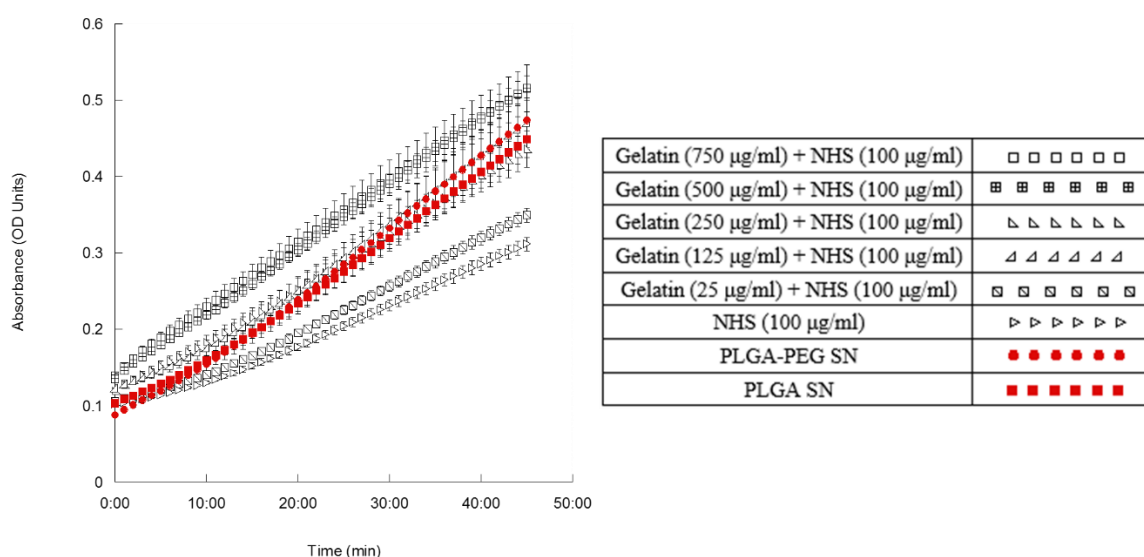| Gelatin (750 µg/ml) + NHS (100 µg/ml) | □ □ □ □ □ □ |
Gelatin (500 µg/ml) + NHS (100 µg/ml)	⊞ ⊞ ⊞ ⊞ ⊞ ⊞
Gelatin (250 µg/ml) + NHS (100 µg/ml)	◣ ◣ ◣ ◣ ◣ ◣
Gelatin (125 µg/ml) + NHS (100 µg/ml)	◢ ◢ ◢ ◢ ◢ ◢
Gelatin (25 µg/ml) + NHS (100 µg/ml)	⊠ ⊠ ⊠ ⊠ ⊠ ⊠
NHS (100 µg/ml)	▷ ▷ ▷ ▷ ▷ ▷
PLGA-PEG SN	● ● ● ● ● ●
PLGA SN	■ ■ ■ ■ ■ ■

Figure 3: BCA Assay Kinetics of Gelatin Standards with Fixed NHS Concentration. Data was acquired every minute for 45 min and incubated at 37°C for the entire duration. Black shapes represent gelatin standards mixed with a fixed concentration of NHS (100 µg/ml). Red shapes indicate SN samples after EDC/NHS conjugation. Gelatin concentration ranges from 0-750 µg/ml.

3.2 BCA ASSAY CORRECTED WITH GELATIN PRECIPITATION USING COMPAT-ABLE™ PROTEIN ASSAY

To verify the sensitivity of BCA-based gelatin quantification, gelatin was precipitated in pellets using the Compat-Able™ Protein Assay. The purpose of the kit is to remove any interfering substances from the pellet. The SN samples and gelatin standards were precipitated, dissolved in PBS and BCA working reagent, incubated for 2 h at 37°C, and measured for absorbance (Figure 4). This resulted in a concentration of 121.7 ± 15.44 and 166.3 ± 27.40 µg/ml gelatin in PLGA SN and PLGA-PEG SN, respectively. Additionally, the mixture of 100 µg/ml NHS, after being treated with the precipitating reagents, recorded an absorbance similar to that of the PBS blank. Using these results, we matched the concentration calculated through the precipitation method with the sample incubation time that estimated a similar concentration. Absorbance data were analyzed to determine gelatin concentration at each time point from Figure 3. After correcting for NHS interference, it was found that using an incubation time of 20 ± 2 min, the concentration of PLGA SN was 119.0 ± 20.44 µg/ml gelatin and the concentration in PLGA-PEG SN was 168.5 ± 27.51 µg/ml gelatin (Figure 5). By utilizing the NHS correction in the BCA assay, the conjugation percentage of the SN samples was calculated at $50.71 \pm 10.10\%$ and $31.76 \pm 10.41\%$ for PLGA SN and PLGA-PEG SN, respectively (Table 1). A comparison of the effect of the incubation time on the calculated conjugation percentage was examined (Figure 6). Adjusting the incubation time, at 37°C, from 30 to 20 min provided a 23% difference in calculated conjugation percentage. This correlates to a calculated conjugation percentage of 50.7% and 62.4% at 20 and 30 min, respectively for PLGA SN. The data at 20 min corresponds to the concentration and conjugation percentage determined using the precipitation assay, which

indicates why adjusting the incubation time is vital in protein estimation procedures. The

data at 20, 30, and 45 min have relatively large standard deviations because data is the

average of three independent experiments which have widely varying conjugation

percentages due to minor variations in experimental conditions such as pH, particle mass,

or gelatin standard concentration. The error bars at 5 min are relatively small because at

this time the BCA assay has not had sufficient time to saturate the sample with color and

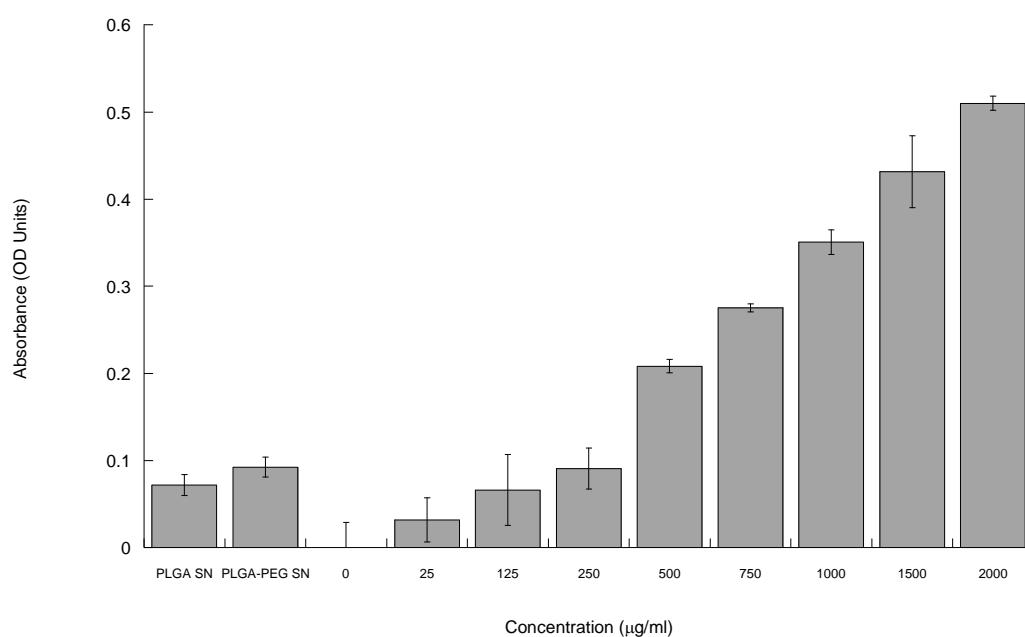create significant distinctions across different concentrations of protein.

Figure 4: Precipitation Assay. Gelatin standard curve data derived after precipitating
gelatin protein from PBS solution using Compat-Able Protein Assay Kit. After
precipitation, samples were diluted in sample volume used and vortexed to dissolve
pellet. All samples were incubated for 2 h at 37°C and measured immediately using BCA
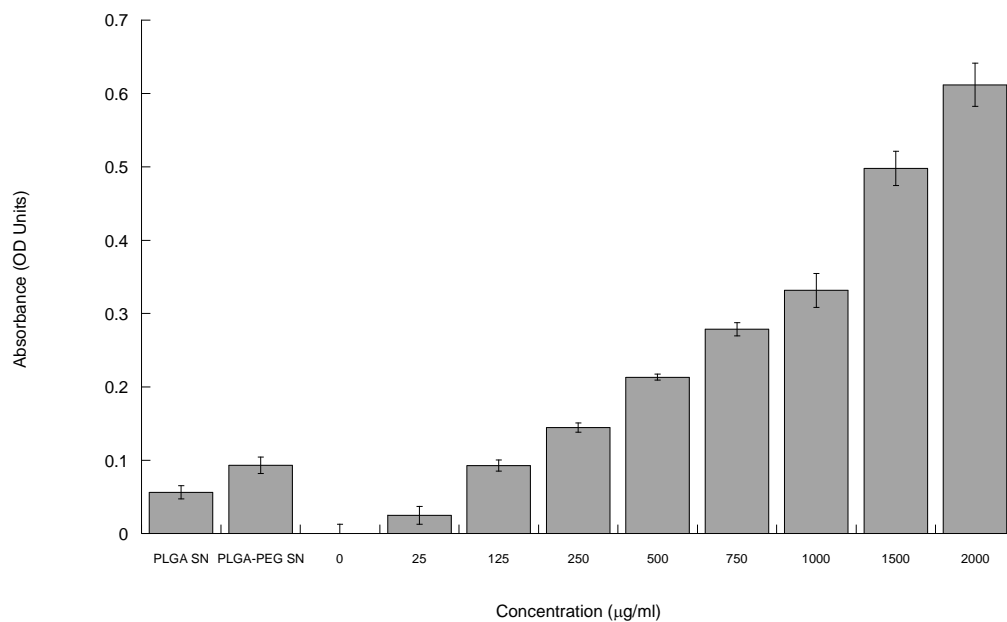assay.

Figure 5: BCA Assay Incorporating NHS Correction. All standards and samples were incubated at 37°C for 20 min and followed the standard BCA assay. Data represent blank corrected absorbance. SN samples were further corrected by subtracting the absorbance of a 100 μg/ml NHS in PBS mixture.

Table 1: Percent Protein Conjugation in SN Sample after NHS Correction. Concentration was calculated using a standard curve constructed from absorbance measurements of blank-corrected gelatin standards. Total mass was determined by multiplying concentration by SN volume. Total gelatin used in the experiment was 740 μg. All samples were incubated at 37°C for 20 min and subsequently measured for absorbance at 562 nm using the BCA assay.

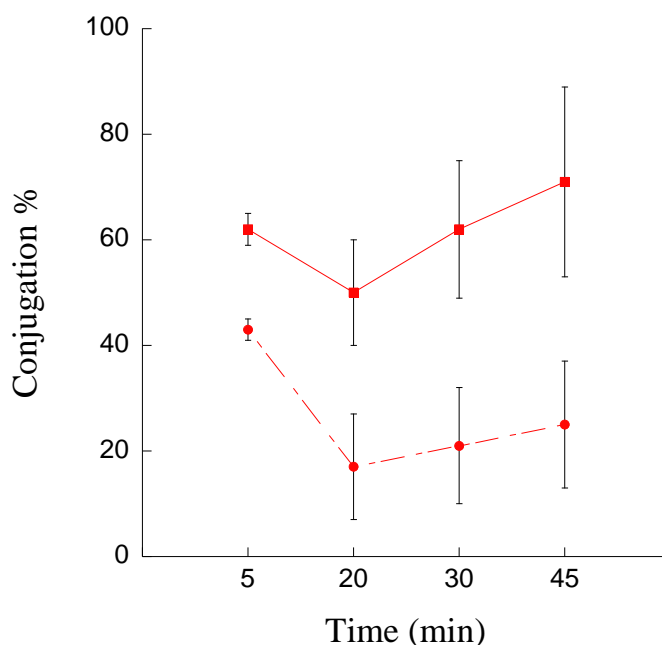| Sample	SN Concentration Precipitated (μg/ml)	SN Concentration BCA Assay (μg/ml)	Conjugation %
PLGA SN	121.7 ± 15.44	119.0 ± 20.44	50.71 ± 10.10
PLGA-PEG SN	166.3 ± 27.40	168.5 ± 27.51	31.76 ± 10.41

Figure 6: Effect of Incubation Time on Protein Estimation. Results represent average calculated conjugation percentage of three experiments after 5, 20, 30, and 45 min of incubation at 37°C for PLGA (■) and PLGA-PEG (●) SNs. Error bars represent mean ± s.d.

It is thus important to check how extreme the conjugation percentage is distorted over varying incubation time. Finally, conjugation percentages were verified using the precipitation assay.

3.3 DISCUSSION

Conducting the assay on a sample containing NHS proposes several problems [18, 19]. NHS reduces the BCA reagent in the same manner as proteins, but the effect is not additive [18]. Additionally, NHS interference is dependent on incubation time, pH, protein concentration, and protein composition due to the nature of the BCA assay [20]. The BCA assay is protein specific in that different proteins will produce different levels of absorbance [6, 16]. For coupling of gelatin on the surface of poly(lactic-*co*-glycolic)

acid (PLGA) microparticles, the standard amine coupling includes a three-step reaction with EDC/NHS chemistry. Upon application of the BCA protein assay, it was found that the SN samples reported absorbance measurements much higher than standards of known concentration (Figure 7a). The undiluted sample measured an absorbance value almost twice as large as the highest protein standard, however, a 50 times dilution (50x dil.) of the sample led to an absorbance value within the standards' range. These results were used to calculate the conjugation efficiency of the EDC/NHS conjugation reaction (Table 2). Sample concentrations were calculated using a best-fit curve correlation derived from the standards' data (Figure 8). The total amount of gelatin used in the experiment was 25 mg, however, the lowest calculated amount of gelatin in the supernatant was 90 mg, almost four times as high. To ensure that the tested sample was not an outlier, EDC/NHS reaction was performed without gelatin. The supernatant of the conjugation sample was collected and absorbance was measured (Figure 7b). This EDC/NHS control (without gelatin) showed higher absorbance than the standards and SNs. Thus, we hypothesized that NHS must be interfering with the BCA reaction [18].

Table 2: Percent Protein Conjugation of SN Sample

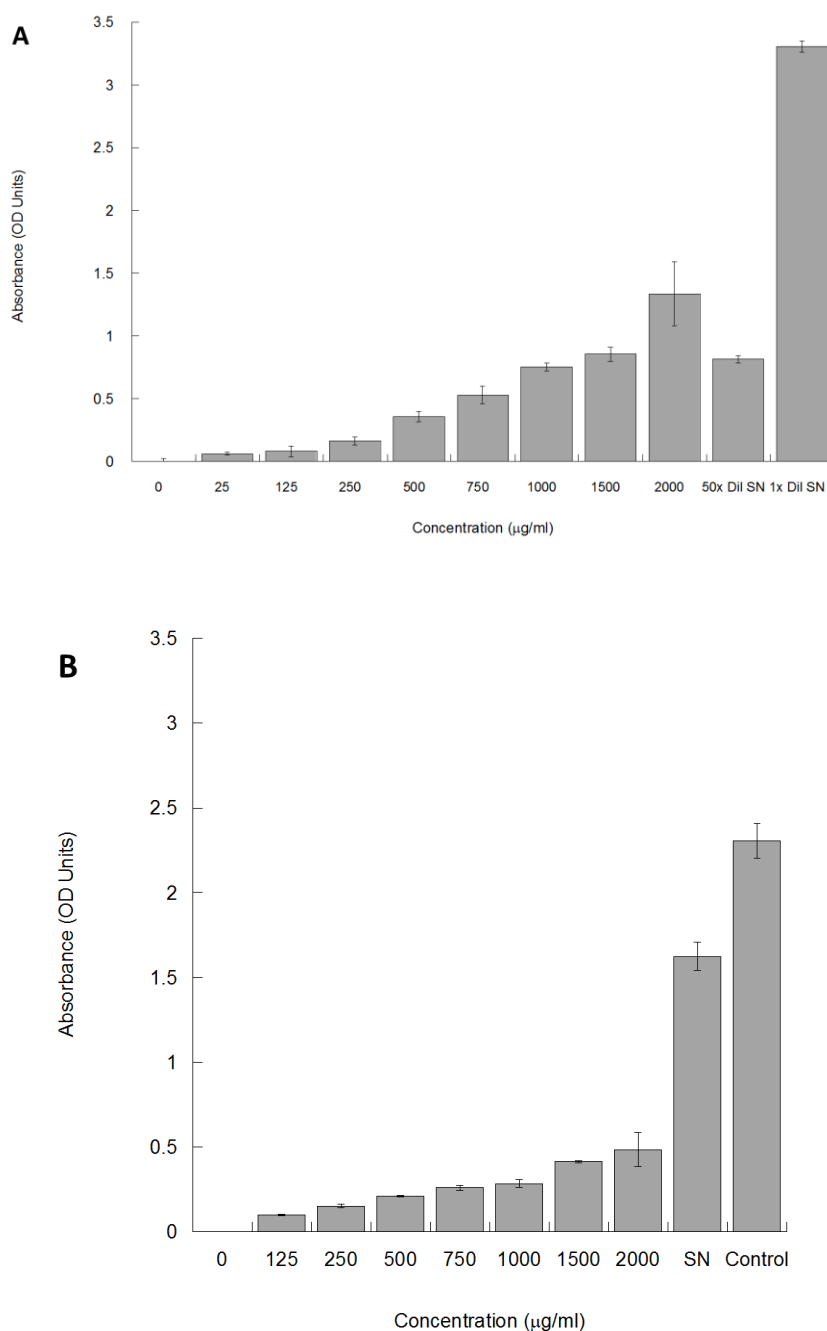| Dilution	SN Concentration (µg/ml)	SN Vol (ml)	SN Gelatin (µg)	Total Gelatin (µg)	Conjugation %
1	5001 ± 70.34	18	90030 ± 1266	25,000	-260.1 ± 5.06
2	5736 ± 54.89	18	103200 ± 1976	25,000	-313 ± 7.90
5	9543 ± 102.8	18	171800 ± 9253	25,000	-587 ± 37.01
10	16230 ± 105.1	18	292100 ± 18910	25,000	-1068 ± 75.66
50	61630 ± 41.77	18	1109000 ± 37600	25,000	-4337 ± 150.4

Figure 7: Initial BCA Assay Results. (A) BCA Assay results with gelatin standards (0-2000 µg/ml) and supernatant samples. All samples were incubated at 37°C for 2 h. SN = undiluted supernatant sample. 50x Dil = SN diluted at a 50:1 PBS:SN ratio. (B) BCA Assay results with standards and samples incubated at 37°C for 30 min. Control consists of a "blank" EDC/NHS conjugation reaction that contained no gelatin protein or PLGA particles. SN = undiluted supernatant sample.

Measurements of conjugation samples following the standard procedure like the BCA assay are challenging. A plethora of interferences can lead to an erroneous composition of the sample supernatant. If one or several of the interfering factors happen(s) to have an impact on measurement accuracy, this biasing effect(s) evolve gradually without any indication in the signal-over-time-curve, leading to significant errors [21, 22]. To detect such errors, thorough method qualification over time must be followed to conclude the total protein determination in bioconjugation engineering. There is thus a substantial need for refined analytical protocols that allow for taking such factors into account, yet without increasing operator workload beyond a reasonable extent. Against this backdrop, the aim of this study was to evaluate and illustrate the impact of NHS on gelatin quantification *via* the BCA assay, as well elucidate a rapid and generally applicable method to compensate for the biasing effects.
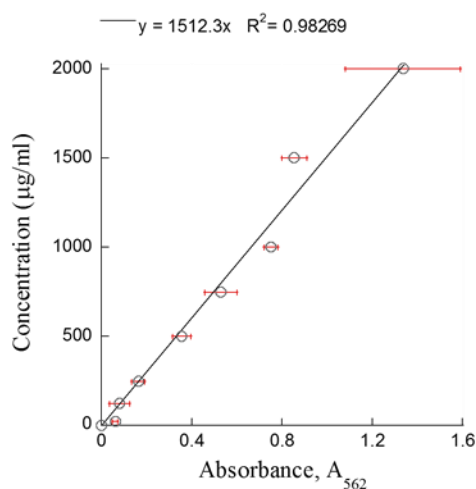

Figure 8: Gelatin standard curve using BCA assay (37°C/ 2h incubation).

The incubation time to accurately estimate gelatin concentration in SN samples varied significantly between PLGA SN and PLGA-PEG SN after initial analysis. However, upon application of the suggested modification to the BCA assay protocol, the PLGA-PEG SN estimation was satisfactory after 20 min of incubation time. The incubation time varied for PLGA-PEG SN samples initially due to PLGA-PEG particles being aspirated during washing and being present in the PLGA-PEG SN. These particles are saturated with NHS esters that are bound to carboxylic acid groups on either the gelatin protein or particles themselves [23]. This NHS ester hydrolyzes within minutes to several hours depending on the pH of the solution [24]. When the ester bond hydrolyzes, the NHS concentration in the SN sample increases which causes a higher absorbance measurement to be read leading to lower conjugation percentages and a skewed determination of necessary incubation time. Preventing particle aspiration into the SN is of paramount importance to accurate protein concentration estimation.

The BCA Assay gives an overestimated value when a sample contains NHS. The sample emits a much darker purple color than any of the standards, even when it is known that the sample has a lower concentration of protein. Quantitatively, the measured absorbance of the samples containing NHS is larger than any of the standards. When calculating the concentration of the sample using the standard curve correlation, the sample protein concentration is estimated far past the range of the standard curve. When calculating total protein content in the sample (multiplying calculated concentration by total supernatant volume) the result is significantly higher than the original starting amount. The inaccuracy in the results is due to the interactions between the protein, NHS, and the BCA assay reagents. Multiple mechanisms are believed to induce the strong

interference of NHS with the BCA assay. One of the proposed mechanisms is that NHS directly reduces the cupric ion (Cu^{2+}) present in the BCA working reagent into the cuprous ion (Cu^+) which participates in the colorimetric chelation reaction [25]. Another proposed mechanism is an esterification reaction between NHS and free protein in the sample, which is part of the protein conjugation reaction [23]. This esterification reaction is thought to prevent free protein in the sample from reducing the Cu^{2+} ion to the Cu^+ ion and subsequently block the colorimetric reaction. This effect is more pronounced at higher protein concentrations (Figure 4). For this reason, the NHS interference in the assay is not additive and is dependent on protein concentration. The reaction kinetics in response to the BCA working reagent of NHS and gelatin differ (Figure 2), which creates the issue with appropriate incubation time. Additionally, the ability for gelatin to induce a color response to the BCA reagent is significantly low which creates even more difficulty in correcting for NHS interference (Figure 2). This weak response to the BCA reagent is due to the low content of cysteine, cystine, tryptophan, and tyrosine amino acids in gelatin, which are known to reduce the Cu^{2+} ion [26-28]. Since NHS interference increases with time and varies depending on protein concentration, a unique method must be employed to correct samples being tested after an EDC/NHS reaction. The method proposed for correcting NHS interference is to perform the BCA Assay using standards composing of the protein being investigated as well as creating an NHS blank. Following 20 min incubation time and absorbance measurements at 562 nm, the NHS absorbance must be subtracted from all unknowns before calculating concentrations using the standard curve.

There are other methods such as a precipitation assay being a useful method for removing interfering substances. However, the precipitation assay has the potential to produce abnormal results and requires several iterations to realize a meaningful result. Additionally, with low concentrations, the protein pellet formed is so small that it can easily be lost during the precipitation procedure. Additionally, this assay adds a significant amount of work to the researcher because all standards and experimental samples must be precipitated and then analyzed using the quantitative assay in question.

The Bradford method is another example. However, there are other proteins/substances that do not respond well to the Bradford method and are better analyzed using the BCA assay. Gelatin is one of the proteins that does not have a strong response to the Bradford method, or rather the Coomassie reagent, unless significant alterations to the assay's protocol are made.

This report is the first time an analysis has been conducted on the response of different concentrations of NHS to the BCA assay and the effect NHS has on the BCA assay. This is important because it shows that certain substances can interact with the assay in such a way that the interference can go undetected. This is because when a sample subject to the BCA assay consists of both protein and NHS, there are competing reactions between NHS and the protein to reduce the cupric ion to the cuprous ion. This competing nature results in a masking of the actual nature of the protein since NHS will inhibit the reduction of the cupric ion by binding to the protein in an esterification reaction, but also reducing the cupric ion to cuprous. This phenomenon has been reported, however, accurate and detailed corrections for this phenomenon have not been thoroughly investigated until now.

4. CONCLUSIONS

The BCA assay is subjected to immense interference by NHS due to Cu^{2+} reduction as well as esterification with free protein in the sample such that even a concentration of 100 μg/ml induces large deviations. It is important to note that when conducting the BCA assay after a conjugation reaction involving NHS, NHS concentration in the sample is less than that originally used in the reaction. Using an NHS blank in tandem with the BCA assay standards provides a suitable correction in protein concentration estimation. Additionally, adjusting incubation time of the sample to approximately 20 min at 37°C and subtracting the NHS blank provides an accurate estimation of protein in the sample.

REFERENCES

[1]   K. Werengowska-Ciecwierz, M. Wisniewski, A. P. Terzyk, and S. Furmaniak, "The Chemistry of Bioconjugation in Nanoparticles-Based Drug Delivery System," *Advances in Condensed Matter Physics,* 2015.

[2]   T. Laemthong, H. H. Kim, K. Dunlap, C. Brocker, D. Barua, D. Forciniti*, et al.*, "Bioresponsive polymer coated drug nanorods for breast cancer treatment," *Nanotechnology,* vol. 28, Jan 2017.

[3]   J. Cheng, B. A. Teply, I. Sherifi, J. Sung, G. Luther, F. X. Gu*, et al.*, "Formulation of functionalized PLGA-PEG nanoparticles for in vivo targeted drug delivery," *Biomaterials,* vol. 28, pp. 869-76, Feb 2007.

[4]   L. N. Goswami, Z. H. Houston, S. J. Sarma, S. S. Jalisatgi, and M. F. Hawthorne, "Efficient synthesis of diverse heterobifunctionalized clickable oligo(ethylene glycol) linkers: potential applications in bioconjugation and targeted drug delivery," *Organic & Biomolecular Chemistry,* vol. 11, pp. 1116-1126, 2013.

[5]   J. K. Oh, D. J. Siegwart, H.-i. Lee, G. Sherwood, L. Peteanu, J. O. Hollinger*, et al.*, "Biodegradable Nanogels Prepared by Atom Transfer Radical Polymerization as Potential Drug Delivery Carriers: Synthesis, Biodegradation, in Vitro Release, and Bioconjugation," *Journal of the American Chemical Society,* vol. 129, pp. 5939-5945, 2007/05/01 2007.

[6]   W. N. Reichelt, D. Waldschitz, C. Herwig, and L. Neutsch, "Bioprocess monitoring: minimizing sample matrix effects for total protein quantification with bicinchoninic acid assay," *J Ind Microbiol Biotechnol,* vol. 43, pp. 1271-80, Sep 2016.

[7]   K. L. J. Rhoderick E. Brown, and Kristi J. Hyland, "Protein Measurement Using Bicinchoninic Acid: Elimination of Interfering Substances," *Analytical Biochemistry,* vol. 180, pp. 136-139, January 27 1989.

[8]   J. M. Walker, "The Bicinchoninic Acid (BCA) Assay for Protein Quantitation," in *Basic Protein and Peptide Protocols*, J. M. Walker, Ed., ed Totowa, NJ: Humana Press, 1994, pp. 5-8.

[9]   K. J. Ong, T. J. MacCormack, R. J. Clark, J. D. Ede, V. A. Ortega, L. C. Felix*, et al.*, "Widespread Nanoparticle-Assay Interference: Implications for Nanotoxicity Testing," *PLOS ONE,* vol. 9, p. e90650, 2014

[10]   S. Jung, C.-H. Choi, C.-S. Lee, and H. Yi, "Integrated fabrication-conjugation methods for polymeric and hybrid microparticles for programmable drug delivery and biosensing applications," *Biotechnology Journal,* vol. 11, pp. 1561-1571, 2016.

[11]   C. C. Yu, Y. Hu, J. H. Duan, W. Yuan, C. Wang, H. Y. Xu *, et al.*, "Novel Aptamer-Nanoparticle Bioconjugates Enhances Delivery of Anticancer Drug to MUC1-Positive Cancer Cells In Vitro," *Plos One,* vol. 6, Sep 2011.

[12]   H. J. Chung, H. K. Kim, J. J. Yoon, and T. G. Park, "Heparin Immobilized Porous PLGA Microspheres for Angiogenic Growth Factor Delivery," *Pharmaceutical Research,* vol. 23, pp. 1835-1841, August 01 2006.

[13]   E. Locatelli and M. Comes Franchini, "Biodegradable PLGA-b-PEG polymeric nanoparticles: synthesis, properties, and nanomedical applications as drug delivery system," *Journal of Nanoparticle Research,* vol. 14, p. 1316, November 25 2012.

[14]   P. M. Valencia, M. H. Hanewich-Hollatz, W. Gao, F. Karim, R. Langer, R. Karnik *, et al.*, "Effects of ligands with different water solubilities on self-assembly and properties of targeted nanoparticles," *Biomaterials,* vol. 32, pp. 6226-6233, 9// 2011.

[15]   T. M. Stich, "Determination of protein covalently bound to agarose supports using bicinchoninic acid," *Analytical Biochemistry,* vol. 191, pp. 343-346, 1990/12/01/ 1990.

[16]   E. G. Hughes, J. L. Maguire, M. T. McMinn, R. E. Scholz, and M. L. Sutherland, "Loss of glial fibrillary acidic protein results in decreased glutamate transport and inhibition of PKA-induced EAAT2 cell surface trafficking," *Molecular Brain Research,* vol. 124, pp. 114-123, 2004/05/19/ 2004.

[17]   R. I. K. P.K. Smith, G.T. Hermanson, A. K. Mallia, F. H. Gartner, M. D. Provenzano, E. K. Fujimoto, N. M. Goeke, B. J. Olson, and D.C. Klenk, "Measurement of Protein Using Bicinchoninic Acid," *Analytical Biohemistry,* vol. 150, pp. 76-85, April 30 1985.

[18]   P. Biotechnology. (2011, User Guide: NHS and Sulfo-NHS.

[19]   S. K. Vashist and C. K. Dixit, "Interference of N-hydroxysuccinimide with bicinchoninic acid protein assay," *Biochem Biophys Res Commun,* vol. 411, pp. 455-7, Jul 29 2011.

[20]   S. K. Vashist, B. Zhang, D. Zheng, K. Al-Rubeaan, J. H. T. Luong, and F.-S. Sheu, "Sulfo-N-hydroxysuccinimide interferes with bicinchoninic acid protein assay," *Analytical Biochemistry,* vol. 417, pp. 156-158, 10/1/ 2011.

[21]   R. L. L. Christine V. Sapan, and Nicholas C. Price, "Colorimetric Protein Assay Techniques," *Biotechnology and Applied Biochemistry,* vol. 29, pp. 99-108, 1999.

[22]   R. E. Morton and T. A. Evans, "Modification of the bicinchoninic acid protein assay to eliminate lipid interference in determining lipoprotein protein content," *Analytical Biochemistry,* vol. 204, pp. 332-334, 1992/08/01/ 1992.

[23] R. J. Kessler and D. D. Fanestil, "Interference by lipids in the determination of protein using bicinchoninic acid," *Analytical Biochemistry,* vol. 159, pp. 138-142, 1986/11/15/ 1986.

[24] M. J. E. Fischer, "Amine Coupling Through EDC/NHS: A Practical Approach," in *Surface Plasmon Resonance: Methods and Protocols*, N. J. Mol and M. J. E. Fischer, Eds., ed Totowa, NJ: Humana Press, 2010, pp. 55-73.

[25] E. T. Gedig, "Chapter 6 Surface Chemistry in SPR Technology," in *Handbook of Surface Plasmon Resonance*, ed: The Royal Society of Chemistry, 2008, pp. 173-220.

[26] A. J. Brenner and E. D. Harris, "A Quantitative Test for Copper Using Bicinchoninic Acid," *Analytical Biochemistry,* vol. 226, pp. 80-84, 1995/03/01/ 1995.

[27] K. J. Wiechelman, R. D. Braun, and J. D. Fitzpatrick, "Investigation of the bicinchoninic acid protein assay: Identification of the groups responsible for color formation," *Analytical Biochemistry,* vol. 175, pp. 231-237, 1988/11/15/ 1988.

[28] J. E. Eastoe, "The amino acid composition of mammalian collagen and gelatin," *Biochemical Journal,* vol. 61, pp. 589-600, 1955.

SECTION

2. CONCLUSIONS

In summary, these investigations have achieved the following outcomes: (1) synthesis of biodegradable PLGA microparticles more than 100 µm in size, (2) successful attachment of HUVEC cells to the surface of these particles, and (3) determining a plausible correction for NHS interference in the BCA assay for protein quantification. These achievements are important in the field of tissue, biological, and chemical engineering, as well as in chemistry. They offer new methodologies for the formulation of bioactive, polymeric materials, as well as provide a new approach to accurately determining the extent of surface modification of these materials. These findings will help future researchers to develop improved models in cellular transport for augmenting tissue response as well as reliable assessment of the characterization of bioactive scaffolds and other materials.

3. FUTURE WORK

In the future, this research can be extrapolated for *in vivo* analysis of cellular delivery *via* microparticle transports. Currently, this research will be extended to an *ex vivo* model consisting of skin tissue samples obtained from The Dermatology Center in Rolla, MO under the supervision of Dr. William V Stoecker in collaboration with the Phelps County Regional Medical Center. Microparticles will be applied to these skin tissue samples and investigated for wound repair augmentation compared to control wound recovery processes. Further, mice or rat models will be used to assess the *in vivo* potential of these microparticles transports. Additionally, other tissues, such as cardiac, bone, or cartilage, could be assessed for repair augmentation using this microparticle system.

Research is currently in progress on polymeric coatings to protect and incorporate cell-covered microparticles for deployment in medical centers and rural or unpopulated areas. Development of a protective polymeric sheath will enable these devices to be transported easily and safely as well as used immediately under any crisis. This will be especially useful in emergency medical situations – emergency medical technicians (EMTs) for example – or in burn victims right at the scene of an incident. Producing technologies of this kind is important, especially in burn victims, as fibrotic scarring and irreparable damage can happen quickly.
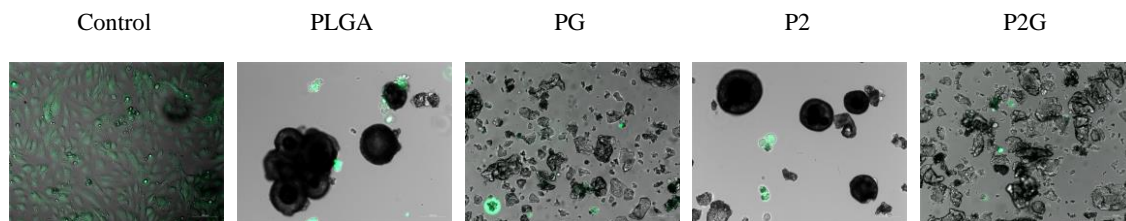
APPENDIX

Control	PLGA	PG	P2	P2G

Figure A.1: HUVECs on microparticles at 8h. HUVEC cells have noticeably started to stop associating with particles and not attach as well across all formulations. However, cells still maintain viability.
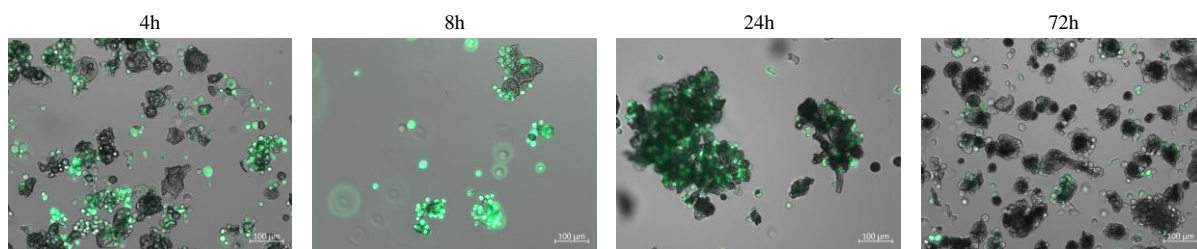
4h	8h	24h	72h

Figure A.2: PLGA-PLL (P2) particles seeded with MDA-MB-231 breast cancer cells. At 4, 8, and 24 hours, cells are noticeably attached to particles and viable, indicated by green fluorescence. At 72h, many cells attached to particles do not fluoresce indicating that these cells have lost viability and are undergoing apoptosis.
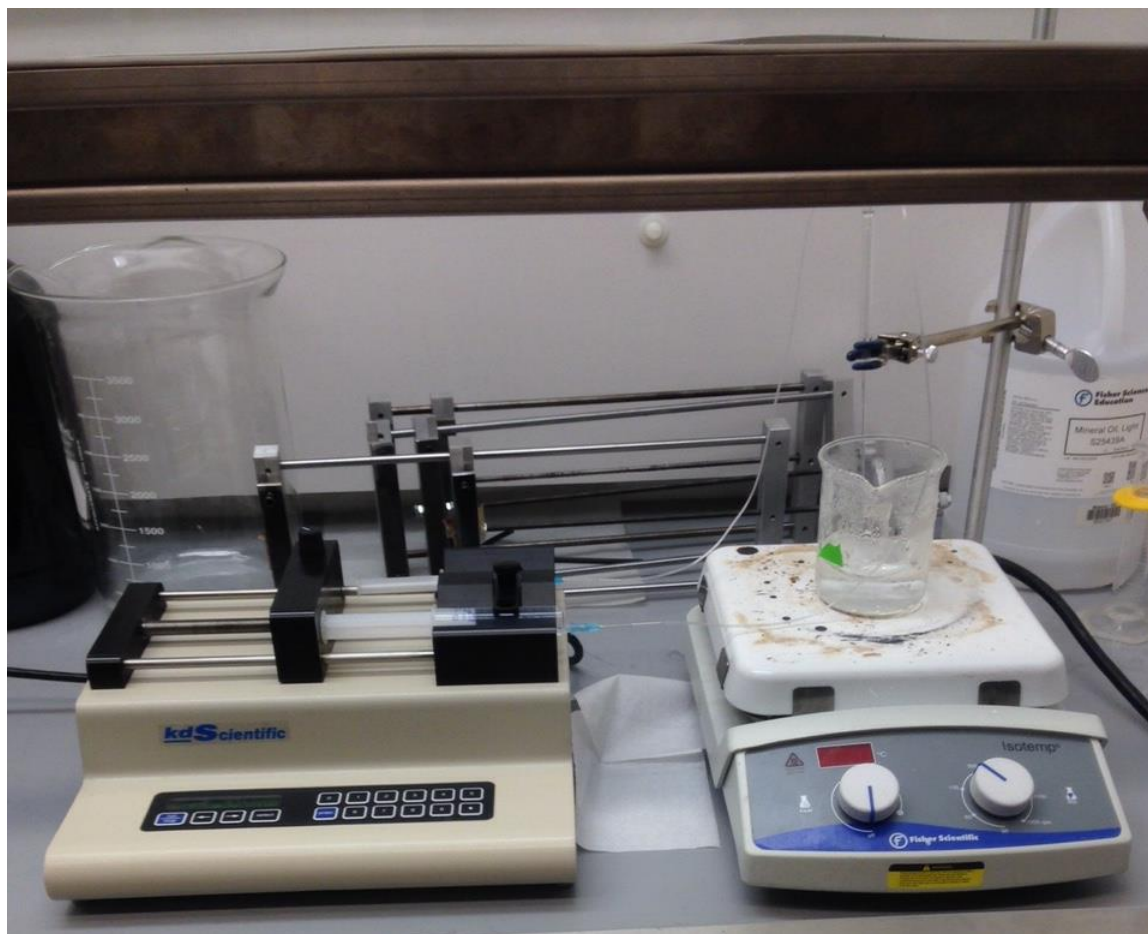
Figure A.3: Overview of microparticle synthesis setup with flow-focusing device.
Two syringes are connected to tygon tubing through a needle, which is threaded through
a glass pasteur pipet. One 10 ml syringe and one 5 ml syringe is used, the former
containing a 1% PVA carrier stream and the latter containing the organic stream
comprised of PLGA and ethyl acetate. The organic stream tubing is threaded to the neck
of the pipet to facilitate formation of droplets whereas the carrier stream is left at the
mouth of the pipet.

REFERENCES

[1]   M. P. Lutolf and J. A. Hubbell, "Synthetic biomaterials as instructive extracellular microenvironments for morphogenesis in tissue engineering," *Nat Biotechnol,* vol. 23, pp. 47-55, Jan 2005.

[2]   P. Gentile, V. Chiono, I. Carmagnola, and P. V. Hatton, "An Overview of Poly(lactic-co-glycolic) Acid (PLGA)-Based Biomaterials for Bone Tissue Engineering," *International Journal of Molecular Sciences,* vol. 15, pp. 3640-3659, 02/28

[3]   R. Havaldar, S. C. Pilli, and B. B. Putti, "Insights into the effects of tensile and compressive loadings on human femur bone," *Advanced Biomedical Research,* vol. 3, p. 101, 03/25

[4]   J. M. Mansour, "Biomechanics of cartilage," in *Kinesiology: The Mechanics and Pathomechanics of Human Movement: Second Edition*, ed, 2013, pp. 69-83.

[5]   K. Kono, S. Kimura, and Y. Imanishi, "pH-Dependent interaction of amphiphilic polypeptide poly(Lys-Aib-Leu-Aib) with lipid bilayer membrane," *Biochemistry,* vol. 29, pp. 3631-3637, 1990/04/17 1990.

[6]   L. Lao, H. Tan, Y. Wang, and C. Gao, "Chitosan modified poly(L-lactide) microspheres as cell microcarriers for cartilage tissue engineering," *Colloids Surf B Biointerfaces,* vol. 66, pp. 218-25, Oct 15 2008.

[7]   K. Werengowska-Ciecwierz, M. Wisniewski, A. P. Terzyk, and S. Furmaniak, "The Chemistry of Bioconjugation in Nanoparticles-Based Drug Delivery System," *Advances in Condensed Matter Physics,* 2015.

[8]   J. Yang, J. Bei, and S. Wang, "Enhanced cell affinity of poly (d,l-lactide) by combining plasma treatment with collagen anchorage," *Biomaterials,* vol. 23, pp. 2607-2614, // 2002.

[9]   A. M. Pereira, R. Machado, A. da Costa, A. Ribeiro, T. Collins, A. C. Gomes*, et al.*, "Silk-based biomaterials functionalized with fibronectin type II promotes cell adhesion," *Acta Biomaterialia,* vol. 47, pp. 50-59, 2017/01/01/ 2017.

[10]   J.-E. Lee, J.-C. Park, Kwang H. Lee, Sang H. Oh, and H. Suh, "Laminin Modified Infection-Preventing Collagen Membrane Containing Silver Sulfadiazine–Hyaluronan Microparticles," *Artificial Organs,* vol. 26, pp. 521-528, 2002.

[11]   S. Barua, J. Ramos, T. Potta, D. Taylor, H.-C. Huang, G. Montanez*, et al.*, "Discovery of Cationic Polymers for Non-viral Gene Delivery using Combinatorial Approaches," *Combinatorial chemistry & high throughput screening,* vol. 14, pp. 908-924, 2011.

[12]   L. Chronopoulou, M. Massimi, M. F. Giardi, C. Cametti, L. C. Devirgiliis, M. Dentini*, et al.*, "Chitosan-coated PLGA nanoparticles: a sustained drug release strategy for cell cultures," *Colloids Surf B Biointerfaces,* vol. 103, pp. 310-7, Mar 01 2013.

[13]   S. Fischer, C. Foerg, S. Ellenberger, H. P. Merkle, and B. Gander, "One-step preparation of polyelectrolyte-coated PLGA microparticles and their functionalization with model ligands," *J Control Release,* vol. 111, pp. 135-44, Mar 10 2006.

[14]   R. A. Quirk, W. C. Chan, M. C. Davies, S. J. B. Tendler, and K. M. Shakesheff, "Poly(l-lysine)–GRGDS as a biomimetic surface modifier for poly(lactic acid)," *Biomaterials,* vol. 22, pp. 865-872, 2001/04/01/ 2001.

[15]   E. Ruoslahti, "RGD AND OTHER RECOGNITION SEQUENCES FOR INTEGRINS," *Annual Review of Cell and Developmental Biology,* vol. 12, pp. 697-715, 1996/11/01 1996.

[16]   B. S. Jacobson and D. Branton, "Plasma membrane: rapid isolation and exposure of the cytoplasmic surface by use of positively charged beads," *Science,* vol. 195, p. 302, 1977.

[17]   B. Tyler, D. Gullotti, A. Mangraviti, T. Utsuki, and H. Brem, "Polylactic acid (PLA) controlled delivery carriers for biomedical applications," *Advanced Drug Delivery Reviews,* vol. 107, pp. 163-175, 2016/12/15/ 2016.

[18]   S. Barua, J. W. Yoo, P. Kolhar, A. Wakankar, Y. R. Gokarn, and S. Mitragotri, "Particle shape enhances specificity of antibody-displaying nanoparticles," *Proceedings of the National Academy of Sciences of the United States of America,* vol. 110, pp. 3270-3275, Feb 26 2013.

[19]   H. Chen, Y. Peng, S. Wu, and L. P. Tan, "Electrospun 3D Fibrous Scaffolds for Chronic Wound Repair," *Materials (Basel),* vol. 9, Apr 6 2016.

[20]   F. Meyer, J. Wardale, S. Best, R. Cameron, N. Rushton, and R. Brooks, "Effects of lactic acid and glycolic acid on human osteoblasts: A way to understand PLGA involvement in PLGA/calcium phosphate composite failure," *Journal of Orthopaedic Research,* vol. 30, pp. 864-871, 2012.

[21]   J. Yu, A.-R. Lee, W.-H. Lin, C.-W. Lin, Y.-K. Wu, and W.-B. Tsai, "Electrospun PLGA Fibers Incorporated with Functionalized Biomolecules for Cardiac Tissue Engineering," *Tissue Engineering. Part A,* vol. 20, pp. 1896-1907, 06/10

[22]   W. Wang, B. Cao, L. Cui, J. Cai, and J. Yin, "Adipose tissue engineering with human adipose tissue-derived adult stem cells and a novel porous scaffold," *J Biomed Mater Res B Appl Biomater,* vol. 101, pp. 68-75, Jan 2013.

[23]   T. Laemthong, H. H. Kim, K. Dunlap, C. Brocker, D. Barua, D. Forciniti*, et al.*, "Bioresponsive polymer coated drug nanorods for breast cancer treatment," *Nanotechnology,* vol. 28, Jan 2017.

[24]   M. A. Islam, S. Barua, and D. Barua, "A multiscale modeling study of particle size effects on the tissue penetration efficacy of drug-delivery nanoparticles," *BMC Systems Biology,* vol. 11, p. 113, 2017/11/25 2017.

[25]   Z. Ding, J. Chen, S. Gao, J. Chang, J. Zhang, and E. T. Kang, "Immobilization of chitosan onto poly-l-lactic acid film surface by plasma graft polymerization to control the morphology of fibroblast and liver cells," *Biomaterials,* vol. 25, pp. 1059-1067, 2004/03/01/ 2004.

[26]   Y.-L. Chen, H.-P. Lee, H.-Y. Chan, L.-Y. Sung, H.-C. Chen, and Y.-C. Hu, "Composite chondroitin-6-sulfate/dermatan sulfate/chitosan scaffolds for cartilage tissue engineering," *Biomaterials,* vol. 28, pp. 2294-2305, 2007/05/01/ 2007.

[27]   A. J. Leblanc, J. S. Touroo, J. B. Hoying, and S. K. Williams, "Adipose stromal vascular fraction cell construct sustains coronary microvascular function after acute myocardial infarction," *Am J Physiol Heart Circ Physiol,* vol. 302, pp. H973-82, Feb 15 2012.

[28]   G. Yang, Z. Xiao, X. Ren, H. Long, K. Ma, H. Qian*, et al.*, "Obtaining spontaneously beating cardiomyocyte-like cells from adipose-derived stromal vascular fractions cultured on enzyme-crosslinked gelatin hydrogels," *Sci Rep,* vol. 7, p. 41781, Feb 3 2017.

[29]   I. P. Monteiro, A. Shukla, A. P. Marques, R. L. Reis, and P. T. Hammond, "Spray-assisted layer-by-layer assembly on hyaluronic acid scaffolds for skin tissue engineering," *J Biomed Mater Res A,* vol. 103, pp. 330-40, Jan 2015.

[30]   Y. J. Tan, X. Tan, W. Y. Yeong, and S. B. Tor, "Hybrid microscaffold-based 3D bioprinting of multi-cellular constructs with high compressive strength: A new biofabrication strategy," *Sci Rep,* vol. 6, p. 39140, Dec 14 2016.

[31]   M. Bao, Q. Zhou, W. Dong, X. Lou, and Y. Zhang, "Ultrasound-modulated shape memory and payload release effects in a biodegradable cylindrical rod made of chitosan-functionalized PLGA microspheres," *Biomacromolecules,* vol. 14, pp. 1971-9, Jun 10 2013.

[32]   H. Tan, D. Huang, L. Lao, and C. Gao, "RGD modified PLGA/gelatin microspheres as microcarriers for chondrocyte delivery," *J Biomed Mater Res B Appl Biomater,* vol. 91, pp. 228-38, Oct 2009.

[33]   R. Shaikh, T. R. Raj Singh, M. J. Garland, A. D. Woolfson, and R. F. Donnelly, "Mucoadhesive drug delivery systems," *Journal of Pharmacy and Bioallied Sciences,* vol. 3, pp. 89-100, Jan-Mar

[34]   M. Rinaudo, "Chitin and chitosan: Properties and applications," *Progress in Polymer Science,* vol. 31, pp. 603-632, 2006/07/01/ 2006.

[35]   D. S. Hwang, S. B. Sim, and H. J. Cha, "Cell adhesion biomaterial based on mussel adhesive protein fused with RGD peptide," *Biomaterials,* vol. 28, pp. 4039-46, Oct 2007.

[36]   G. Li, J. Chen, X. Zhang, G. He, W. Tan, H. Wu, *et al.*, "Cardiac repair in a mouse model of acute myocardial infarction with trophoblast stem cells," *Sci Rep,* vol. 7, p. 44376, Mar 15 2017.

VITA

Daniel Lee Smith was born in St. Louis, Missouri. In the summer of 2009, he attended the Missouri Scholars Academy at the University of Missouri – Columbia. In May 2011, he graduated from Mehlville Senior High School, St. Louis, Missouri, as Salutatorian. In May 2015, he received his B.S. in Chemical Engineering (Biochemical emphasis) from the University of Missouri – Columbia, Columbia, Missouri. He worked for Vulcan Systems as a Chemical Engineer for 9 months before enrolling as a Master's Thesis student. While pursuing his M.S., he volunteered with Mentoring Makes a Difference, a local mentoring program which fosters improving the lives of underserved children. In May 2018, he received his M.S. in Chemical Engineering from the Missouri University of Science and Technology, Rolla, Missouri.